THE JOURNAL

OF THE

AMERICAN CERAMIC SOCIETY

JANUARY 1, 1944

MONTHLY PUBLICATION DEVOTED TO THE ARTS AND SCIENCES RELATED TO THE SILICATE INDUSTRIES

TABLE OF CONTENTS

Vol. 27 January 1, 1944 No. 1

THE JOURNAL

Some Particulate Characteristics of Commercial Flint and Feldspar..... 1–7
By R. Russell, Jr., and R. S. Weisz

Brucite Magnesia..... 8–10
By M. F. Goudge

Changes of Properties of Glass Resulting From Changes of Composition..... 10–12
By Maurice L. Huggins and Kuan-Han Sun

Glass Properties and the Periodic Table..... 13–17
By Maurice L. Huggins and Kuan-Han Sun

Fundamental Properties of Soluble Salts in Enamel Mill Liquors..... 17–24
By M. K. Blanchard and A. I. Andrews

Enamel Film Strength as Affected by Properties of Enamel Before, During, and After Drying. 25–31
By M. K. Blanchard and A. I. Andrews

Publication Office: 20th & Northampton Sts., Easton, Pa.
Editorial Office: 2525 N. High St., Columbus 2, Ohio
Committee on Publications: J. D. SULLIVAN, *Chairman;* H. H. BLAU, R. L. STONE, J. J. CANFIELD, H. THIEMECKE, AND R. C. PURDY, *ex officio.*
Entered as second-class matter at the post office at Easton, Pa., under the act of March 3, 1879. Published monthly.
Subscription fifteen dollars ($15.00) a year. Single numbers $1.50
(Foreign and Canadian postage, 50¢ additional on subscriptions)
(Copyright 1944, American Ceramic Society, Inc.)

THE JOURNAL
OF
THE AMERICAN CERAMIC SOCIETY

Volume 27 January 1, 1944 Number 1

SOME PARTICULATE CHARACTERISTICS OF COMMERCIAL FLINT AND FELDSPAR*

By R. Russell, Jr., and R. S. Weisz

Abstract

The particle-size variations of eleven shipments of commercial flint and of fifteen shipments of feldspar have been investigated as a possible cause of production variations in electrical porcelain. A correlation of sieve data with specific surface calculations based on sedimentation determinations was made on six grades of commercial flint. The Andreasen pipette sedimentation method was used for all tests except those in which the hydrometer method was employed for comparison purposes. Either of these sedimentation methods had adequate accuracy to control particle size. The percentage remaining on the 325-mesh sieve, however, could not be correlated with the specific surface values. Particle-size distribution was determined for each sample. To facilitate comparisons, specific surface values were calculated from a plot of the distribution data on log-probability graph paper. The investigation included the effect of various liquid suspending media and electrolytes on the settling characteristics of flint and feldspar. Neither flint nor feldspar could be adequately dispersed in nonpolar liquids. Feldspar apparently has surface-active characteristics that permit it to be flocculated or deflocculated, depending on the nature of the ions present in solution. An anomalous peptizability of some feldspar samples in the particle-size range below 3 microns is discussed.

I. Introduction

The quality of ceramic ware depends in part on the uniformity of the constituent raw materials. Particle-size distribution of the nonplastic constituents, such as flint, feldspar, and nepheline syenite, is therefore important.

High-temperature reactions resulting in the vitrification of ceramic ware are not instantaneous but depend on both time and temperature, and the rate of these reactions is materially affected by the particle-size distribution of the constituents.

Geller, Evans, and Creamer[1] studied the effect of flint and feldspar fractions which varied in grain size from less than 10 microns to from 35 to 75 microns, that is, relative specific surfaces of 7500 to 450 sq. cm. per gm. Promising commercial possibilities were concluded to exist for the lower temperature vitrification of whiteware bodies made of finely ground materials.

Krause,[2] using various fractions of quartz grading from 0 to 15 microns up to 60 to 75 microns, observed that the best characteristics were obtained with a grain-size fraction of 15 to 30 microns.

Parmelee and Morgan,[3] who studied bodies containing flint of varying average grain size obtained by blending coarse and fine fractions, found proportionate effects on vitrification as the average particle size was progressively decreased from 45 to 10 microns.

Harkort[4] has stated that the finer the quartz the greater is its influence on contraction and expansion properties of the body as a result of its more intimate association with the other body ingredients. Geller,

---

* Presented at the Forty-Fifth Annual Meeting, The American Ceramic Society, Pittsburgh, Pa., April 20, 1943 (White Wares Division). Received August 26, 1943.

[1] R. F. Geller, D. N. Evans, and A. S. Creamer, "Effects of Particle Size of a Potter's Flint and Feldspar in Whiteware," *Bur. Standards Jour. Research*, **11** [3] 327–40 (1933); R. P. 594; *Ceram. Abs.*, **12** [12] 427 (1933).

[2] Otto Krause, "Relationships Between Grain Size of Quartz and Properties of Hard Porcelain, I–II," *Sprechsaal*, **70** [49] 611–12; [50] 623–25; [51] 633–35; [52] 647–48 (1937); *Ceram. Abs.*, **17** [6] 224 (1938).

[3] C. W. Parmelee and W. R. Morgan, "Effect of Fineness of Flint on Vitrification of a Ceramic Body," *Ceram. Ind.*, **22** [3] 146–52 (1934); *Ceram. Abs.*, **13** [5] 125 (1934).

[4] H. Harkort, "Effect of Particle Size of Quartz on Properties of Whiteware Bodies," *Ber. deut. keram. Ges.*, **9** [8] 476–89 (1928); *Ceram. Abs.*, **7** [12] 844 (1928).

Evans, and Creamer[1] and Koenig[5] also observed this increased body thermal expansion as the fineness of quartz was increased. The particle-size effects of flint were relatively more pronounced than those of feldspar in the bodies tested. Koenig also found considerable variation in the grain-size distribution of different shipments of commercial flint and feldspar and suggested that closer control might be warranted. Numerous other references on the subject, some of which date back over forty years, were listed in Koenig's report.

In addition to the effect in bodies of the particle-size distribution of the nonplastics, the effect of fineness on the properties of glazes, stains, and enamels has been extensively investigated as shown by the list of references compiled by Koenig and Henderson.[6]

The primary objectives of this investigation were to devise a means for the laboratory determination and comparison of particle-size distributions of commercial shipments of flint and feldspar, to develop a procedure for the production control of commercial shipments, and to study in general the particulate characteristics of the materials. Similar studies may eventually lead to more specific recommendations as to the particle-size distribution of materials desired and to the adoption of specifications limiting permissible deviations.

II. Methods for Particle-Size Determination

The various methods of determining particle-size distribution have been classified by Roller[7] and more recently by Schweyer and Work[8(a)] in a symposium on the newer methods of particle-size determination. Comprehensive listings of the literature are included in the published records of this symposium.[8]

A survey of the various methods proposed for the determination of particle size in the subsieve range (1 to 45 μ) indicated that the Andreasen pipette apparatus was the most promising for laboratory use in view of the joint considerations of time and accuracy. This apparatus, as originally designed by Andreasen[9] and modified by others, was used in the manner described for whiteware clays by Loomis.[10] A hydrometer method, however, was believed to be more convenient for plant-control use.

Comparative tests were made accordingly by the pipette method and by a hydrometer method used in the mechanical analysis of soils[11] and devised originally by Bouyoucos.[12]

(1) Andreasen Pipette Method

Loomis[10] has described the Andreasen pipette with detailed instructions for its use. Samples were taken at intervals of 3, 10, and 30 minutes and at 1, 3, and 7 hours. The weights of these samples after drying were calculated as the percentage of the material finer than the corresponding grain size. These grain sizes (diameters) were the same for all samples because the various factors, such as temperature, time, and height of fall, were standardized (it so happens that the densities of flint and feldspar are also nearly the same (2.60 ± 0.02)). The actual diameters were 31.8, 17.4, 9.9, 6.9, 4.0, and 2.6 microns, respectively. Duplicate tests on a given sample usually gave weight percentages which checked within 1%.

(2) Hydrometer Method

The procedure followed for the hydrometer method is that described in the A.S.T.M. Standard Method of Mechanical Analysis of Soils.[13] Fifty grams of the sample were weighed and dispersed in distilled water for about 10 minutes by means of a confectioner's stirrer. The resulting slurry was transferred to a glass graduate (18 in. high and $2^1/_4$ in. in diameter), and distilled water was added until the mixture attained a volume of 1 liter. The graduate was then placed in a constant temperature bath at 30°C. After reaching that temperature, the cylinder was removed and the suspension was uniformly dispersed by rotating through an angle of 180° for one minute. During this operation, the palm of the hand was used as a stopper

[5] J. H. Koenig, "Particle-Size Distribution of Ingredients versus Body Properties," *Bull. Amer. Ceram. Soc.*, **19** [11] 424–30 (1940).

[6] J. H. Koenig and F. C. Henderson, "Particle-Size Distribution of Glazes," *Jour. Amer. Ceram. Soc.*, **24** [9] 286–97 (1941).

[7] P. S. Roller, "Classification of Methods of Mechanical Analysis of Particulate Materials," *Proc. Amer. Soc. Testing Materials*, **37** [Part II] 675–83 (1937).

[8] Symposium on New Methods for Particle-Size Determination in the Subsieve Range, American Society for Testing Materials, Washington Spring Meeting, March 4, 1941; published, Philadelphia, 1941. 120 pp.; *Ceram. Abs.*, **21** [4] 92 (1942).

(*a*) H. E. Schweyer and L. T. Work, "Methods for Determining Particle-Size Distribution," pp. 1–23.

(*b*) P. C. Carman, "Shape and Surface of Fine Powders by the Permeability Method," pp. 24–35.

(*c*) P. S. Roller and P. V. Roundy, Jr., "Surface Area of Portland Cement," pp. 36–51.

(*d*) A. Klein, "Improved Hydrometer for Use in Fineness Determinations," pp. 52–65.

(*e*) S. W. Martin, "Determination of Subsieve Particle-Size Distributions by Sedimentation Methods," pp. 66–89.

(*f*) James Hillier, "Electron Microscope in Determination of Particle-Size Characteristics," pp. 90–91.

(*g*) P. H. Emmett, "New Method for Measuring Surface Areas of Finely Divided Materials and for Determining Size of Particles," pp. 95–106.

(*h*) W. W. Ewing, "Specific Surface of Pigments by Adsorption from Solution," pp. 107–10.

[9] A. H. M. Andreasen, "Grinding of Materials; Theorectical and Experimental Research on Particle-Size Determinations Incident to the Disintegration Process," *Kolloid Beihefte*, **27**, 349–458 (1928); *Ceram. Abs.*, **8** [8] 301 (1929).

[10] G. A. Loomis, "Grain Size of Whiteware Clays as Determined by the Andreasen Pipette," *Jour. Amer. Ceram. Soc.*, **21** [11] 393–99 (1938).

[11] G. J. Bouyoucos, "Comparison Between Pipette Method and Hydrometer Method for Making Mechanical Analyses of Soil," *Soil Sci.*, **38**, 335–43 (1934).

[12] (*a*) G. J. Bouyoucos, "The Hydrometer as a New and Rapid Method for Determining Colloidal Content of Soils," *ibid.*, **23**, 319–30 (1927).

(*b*) G. J. Bouyoucos, "Sensitive Hydrometer for Determining Small Amounts of Clay or Colloids in Soils," *ibid.*, **44**, 245–46 (1937).

[13] American Society for Testing Materials, "Standard Method of Mechanical Analysis of Soils, A.S.T.M. Designation D422–39," *Amer. Soc. Testing Materials*, **39** [Part II] 453–62 (1939).

over the mouth of the graduate. After this final dispersing operation, the cylinder was replaced in the constant temperature bath and the time was recorded. At intervals of 3, 10, 30, and 90 minutes and 3, 6, and 8 hours after the test was started, density readings were taken as follows: The hydrometer was carefully placed in the cylinder 30 seconds before the test time, 15 seconds being required for lowering the hydrometer and 15 seconds for it to come to equilibrium. The top of the meniscus was read in each case, after which the hydrometer was carefully removed, wiped, and placed in the water bath. A reading was taken in the initial trials one minute after the start of the tests, but check determinations showed these readings to be unreliable because the density of the mixture was changing too rapidly.

From each density reading, a maximum diameter of particles remaining in suspension and the corresponding weight percentage may be calculated.[13] The diameters were computed from Stokes' law (equation (1)).

$$d = \sqrt{\frac{18\eta L}{g(D_1 - D_2)t}} \qquad (1)$$

d = max. grain diameter (cm.).
η = coefficient of viscosity of suspending medium (poises).
L = distance through which particles settle in given time (cm.).
t = time (seconds).
D_1 = density of particle.
D_2 = density of medium.
g = acceleration of gravity (cm./sec.^{2}).

In the present investigation, $\eta = 8.00 \times 10^{-3}$ poises (30°C.), g = 980 cm. per sec.^{2}, D_1 = 2.60, and D_2 = 0.998. The expression may therefore be simplified to the form of equation (2).

$$d = 9.58 \times 10^{-3} \sqrt{\frac{L}{t}} \text{ cm.} \qquad (2)$$

The determination of L, the distance through which the particles fall, was not entirely straightforward because the density of the mixture varies with the depth and the time. It has been shown, however, that with the streamlined hydrometers (Fig. 5), L may be taken as the distance from the surface to the center of volume of the hydrometer.[13] This distance may be easily calculated from the dimensions, and a graph (Fig. 1) was prepared which correlated the hydrometer readings with L.

The percentages corresponding to the various grain sizes were calculated according to equation (3).

$$\% = 100\,(R_c - 1)\left(\frac{D_1}{D_1 - D_2}\right)\frac{V}{W} \qquad (3)$$

R_c = corrected hydrometer reading.
D_1 = density of particles (gm./cm.^{3}).
D_2 = density of medium (gm./cm.^{3}).
V = volume of mixture (cc.).
W = weight of sample taken (gm.).

In the present investigation, $D_1 = 2.60$, $D_2 = 0.998$, $V = 1000$, and $W = 50$.

The expression therefore simplifies to equation (4).

$$\% = 3240(R_c - 1) \qquad (4)$$

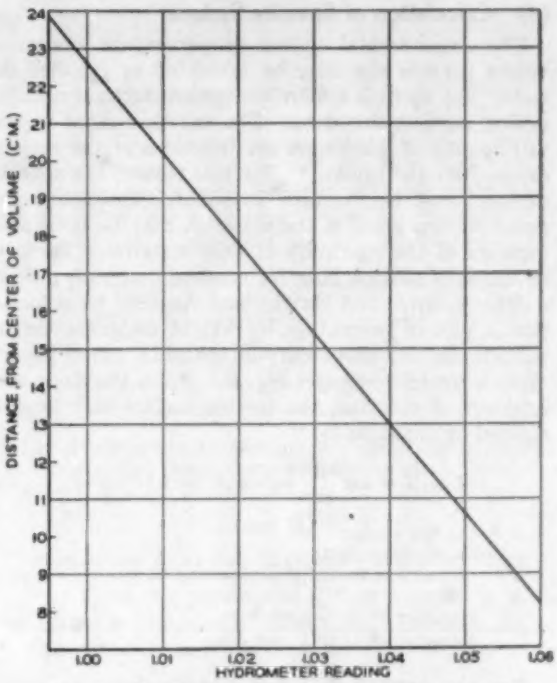

FIG. 1.—Calibration curve for soil hydrometer.

The corrected hydrometer reading, R_c, differed from the actual reading, R, by an amount depending on the temperature of the test and the temperature of calibration of the hydrometer. The hydrometer used was calibrated at 20°C. Inasmuch as the experiments were performed at 30°C., a correction equal to the density of water at 20° minus the density at 30° (0.0026) had to be added to each reading. The correction made in this manner actually did not take into consideration the expansion of the paper scale, but this expansion is undoubtedly a very small source of error. Reimers[14] has mentioned a correction for the rise in liquid level when the hydrometer bulb was inserted. The authors, however, have found this rise to be insignificant with the hydrometer and cylinder used.

(3) Sieve Method

Because control of particle size of the nonplastics is usually conducted by sieve analysis, it was thought advisable to compare the results of the sedimentation tests with those of the sieve tests. The following procedure was therefore adopted for the sieve tests: One hundred grams of the material were dispersed in water by means of the confectioner's stirrer. The sample was wet-sieved through a standard 325-mesh screen and the residue was dried at 110°C., transferred to a tared watch glass, and weighed. The sieving was performed under a gentle stream of tap water until examination showed no appreciable amount of material passing (which usually required 10 to 15 minutes). Check determinations were always made.

[14] J. C. Reimers, "Application of Hydrometer Method of Fineness Analysis to Porcelain Enamel Slips," *Bull Amer. Ceram. Soc.*, **18** [6] 195–200 (1939).

(4) Calculation of Specific Surface

The experimental values of percentage undersize versus particle size may be tabulated or graphed directly, but there is a more convenient method of comparing particle-size data. The reaction rates in the vitrification of whiteware are functions of the surface exposed by the grains.[15] For this reason, the specific surface, that is, the area in square centimeters exposed by one gram of the material, may be used as a measure of the reactivity of that material. The distribution of particle sizes for crushed materials follows a definite law,[16] and Hatch[17] and Austin[18] have found that a plot of percentage by weight undersize versus particle size on "probability-logarithmic" graph paper* gives a straight line (see Fig. 2). From the slope and intercept of this line, the specific surface may be calculated by equation (5).[17]

$$\text{Log } S = \log \frac{a}{Wn} - \log M + 1.15 \log^2 d \qquad (5)$$

S = specific surface.
a and n = shape factors.
W = density of material (2.6 in this case).
M = diameter at 50% undersize.
$d = \dfrac{\text{diameter at 50\% undersize}}{\text{diameter at 15.9\% undersize}}$.

Because crushed flint and feldspar have no particular simple geometric shape, there is considerable uncertainty in assigning values to the factors a and n. Most authors have assumed that the particles are spherical, in which case $a/n = 6$. (a = coefficient of surface-area formula; for a sphere $A = \pi D^2$ or $a = \pi$; n = coefficient of volume formula for a sphere, $V = {}^1/_6\,\pi D^3$ or $n = {}^1/_6\,\pi$; therefore $a/n = 6$ for a sphere.) Martin[19] has experimentally determined $a = 2.1$ and $n = 0.27$ ($a/n = 7.8$) for ground quartz. Andreasen[20] assumed that the particles were cubes of the same volume as the spheres calculated from Stokes' law. This assumption gives $a/n = 7.44$.

Three different values for specific surface of each flint and two different values for specific surface of each feldspar have been included in this paper and have been calculated according to the assumptions that have been described. To compare the results within this investigation, any one of the series may be used; to compare data from different authors, however, the proper series must be chosen.

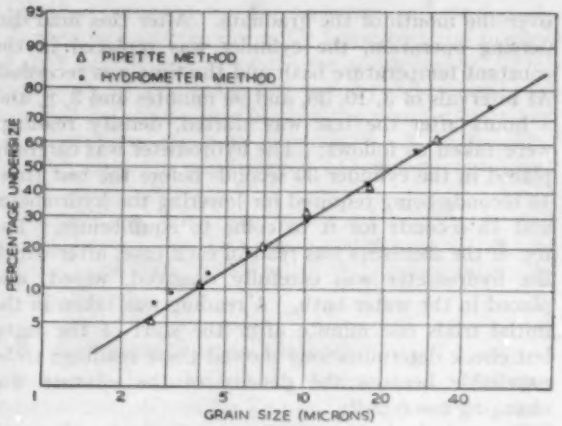

FIG. 2.—Comparison of hydrometer and pipette methods (logarithmic-probability plot).

III. Results of Tests

(1) Tests on Commercial Flint Shipments

The results of this part of the investigation, which include the tests on eleven shipments of a commercial flint, are summarized in Table I. S_1, S_2, and S_3 refer respectively to specific surfaces calculated assuming spheres, Martin's experimental shape, and cubes. The amount of material retained on the 325-mesh sieve is also recorded. No relation exists between sieve data and the specific surfaces.

TABLE I

PARTICLE-SIZE DATA FOR FLINTS

Sample No.	S_1 (cm.²/gm.)	S_2 (cm.²/gm.)	S_3 (cm.²/gm.)	Coarser than 325-mesh (%)
1	2160	2790	2680	7.5
2	2420	3130	3000	7.0
3	2160	2800	2690	9.0
4	2090	2700	2590	6.0
5	2220	2850	2750	8.0
6	2550	3250	3160	7.0
7	2360	3060	2870	8.5
8	2560	3310	3180	7.0
9	2160	2800	2690	7.5
10	2300	2980	2860	5.5
11	2420	3130	3000	10.0

Assuming the particle-size data to be correct to 1% and a reasonable value for errors in obtaining slope and intercept of the curve, the maximum precision of the specific surface values is found to be about 5%. (These limits of precision also apply to other pipette tests listed in subsequent sections.) The average value of S_1 for the 11 samples is 2310 sq. cm. per gm. Because there is a deviation of almost 10% from this average in the maximum and minimum values of S, there is a significant difference in the particle size of different samples supplied as the same grade of flint.

[15] I. Langmuir, "Dissociation of Solids and Kinetic Interpretation of Phase Rule," *Jour. Amer. Chem. Soc.*, **38**, 2263 (1916).

[16] P. S. Roller, "Law of Size Distribution and Statistical Description of Particulate Materials," *Jour. Franklin Inst.*, **223**, 609–33 (1937); *Ceram. Abs.*, **17** [11] 360 (1938).

[17] (*a*) T. Hatch and S. P. Choate, "Statistical Description of Size Properties of Nonuniform Particulate Substances," *Jour. Franklin Inst.*, **207**, 369–87 (1929).
(*b*) T. Hatch, "Determination of Average Particle Size from Screen Analysis of Nonuniform Particulate Substances," *ibid.*, **215**, 27–37 (1933).

[18] J. B. Austin, "Methods of Representing Distribution of Particle Size," *Ind. Eng. Chem., Anal. Ed.*, **11**, 334–39 (1939); *Ceram. Abs.*, **18** [9] 256 (1939).

* Obtained from the Codex Book Co., Inc., Norwood, Mass.

[19] Geoffrey Martin and E. A. Bowes, "Researches on the Theory of Fine Grinding, IX–X," *Trans. Ceram. Soc.* [England], **27**, 247–58, 259–84 (1928).

[20] A. H. M. Andreasen, "Validity of Stokes' Law for Nonspherical Particles," *Kolloid-Z.*, **48**, 175–79 (1929); *Ceram. Abs.*, **9** [1] 66 (1930).

(2) Tests on Standard Grades of Flint

Six grades of flint of varying fineness furnished by a single producer were tested by pipette and sieve analyses. The results are listed in Table II and are shown in Fig. 3, which is a logarithmic-probability plot of the data obtained from the pipette analysis. Sample No. I is listed by the producer as the coarsest and No. VI as the finest. The most striking feature of these data is that, although the "coarse" fractions of the various grades follow the expected order of fineness, some of the distribution curves cross each other. As a result, the values for specific surface do not follow the order of fineness indicated by the producer.

TABLE II

PARTICLE-SIZE DATA FOR DIFFERENT GRADES OF FLINT

Sample No.	S_1 (cm.²/gm.)	S_2 (cm.²/gm.)	S_3 (cm.²/gm.)	Coarser than 325-mesh (%)
I	1740	2260	2160	34.9
II	2810	3640	2200	21.5
III	2970	3840	3690	10.8
IV	2680	3450	3310	9.5
V	3920	5060	4860	4.5
VI	3100	3920	3760	4.4

A more striking argument for the use of subsieve methods for the control of grinding operations could hardly be found. Certainly the sieve data are not sufficient because they cover only a small fraction of the particle-size range.

It was hoped at first that the sieve data could be plotted on the same curve as the sedimentation data. Attempts to do this, however, showed it to be impossible, even if an arbitrary value was assumed for the maximum particle size passed by the sieve. Several factors cause the deviation. Whereas the sedimentation diameters are for particles under this size, the sieve values are for oversize particles. The coarsest fraction of a ground material, furthermore, deviates from the usual distribution law. As Roller[16] states,

> During pulverization, one may assume that, at a given size in the interior of the powder, an equilibrium holds between the rate of loss of particles to the finer sizes and the rate of gain from the coarser sizes. At the coarse end of the curve, this equilibrium is disturbed by the coarsest particles not being replenished at the expected rate because of the discontinuity at the upper limit of size. Hence, the distribution at the coarse end is sparser than it should be.

The seive data for materials as fine as potter's flint are therefore not merely useless in most cases but they may be misleading as well.

(3) Tests on Feldspars and Nepheline Syenite

The results obtained in tests on fifteen feldspar samples and one nepheline syenite are given in Table III. Samples Nos. 1 through 13 are type A feldspar, Nos. 14 and 15 are type B feldspar, and No. 16 is a nepheline syenite. Among the type A feldspars, the maximum and minimum values for S varied respectively by 34% and 31% from the mean for the entire series.

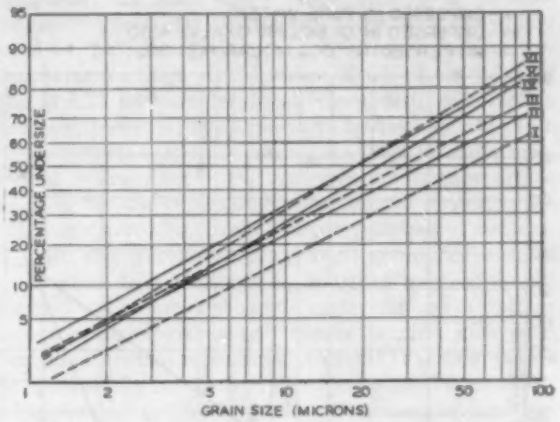

FIG. 3.—Particle-size distribution of six grades of commercial flint (logarithmic-probability plot).

TABLE III

PARTICLE-SIZE DATA FOR FELDSPARS AND NEPHELINE SYENITE

Sample No.	S_1 (cm.²/gm.)	S_2 (cm.²/gm.)	Coarser than 325-mesh (%)
1-A*	3860	4790	5.5
2-A	2510	3120	2.8
3-A	2460	3060	16.0
4-A	3000	3680	5.0
5-A	3260	4050	5.5
6-A	3430	4250	4.0
7-A	3470	4300	4.5
8-A	3900	4850	3.2
9-A	2800	3470	6.0
10-A	2540	3150	7.0
11-A	2360	2930	6.0
12-A	2310	2870	4.5
13-A	2000	2460	8.0
14-B†	3780	4680	6.2
15-B	3900	4850	3.7
16-C‡	6700	8300	6.0

* A, type A feldspar.
† B, type B feldspar.
‡ C, nepheline syenite.

The variation in specific surface in some cases is paralleled by the variation in percentage retained on the 325-mesh sieve; in other cases it is not.

Whereas all of the data for the flint samples gave good straight lines when plotted on logarithmic-probability graph paper, some of the type A feldspars showed significant deviations in the range below 5 microns (see Fig. 4). For reasons to be discussed in section (4), these deviations were ignored in calculating specific surfaces, and the slope was determined from the extrapolated straight line.

(4) Effect of Various Suspending Media on Settling Rates

The settling rate and therefore the apparent particle-size distribution for base-exchanging substances such as clay are known to be strongly affected by electrolytes.[21]

[21] T. D. Baver, Soil Physics. John Wiley & Sons, Inc., New York, 1940. 370 pp.

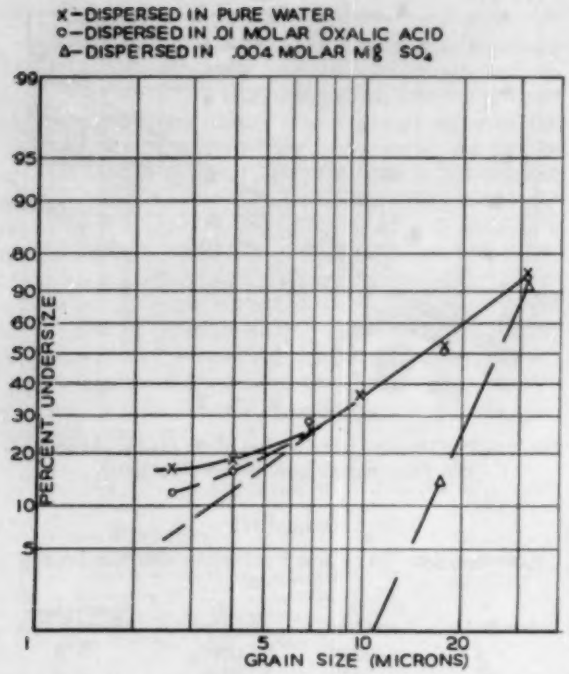

FIG. 4.—Apparent particle-size distribution of type A feldspar.

Kelley and Jenny[22] have also demonstrated that finely ground feldspar shows considerable base-exchange capacity. In view of this fact, a feldspar suspension might be expected to be flocculated or deflocculated, depending on the nature of the ions present. Figure 4 indicates that such behavior was actually found for some of the feldspars. A large majority of the type A feldspars, when suspended in distilled water, showed a tendency for the particles smaller than 5 microns not to settle out or to settle out more slowly than expected from Stokes' law. The example chosen for Fig. 4 was an extreme case; most samples deviated less noticeably from a straight line. With a solution only 0.004 molar in magnesium sulfate, the same feldspar settled out completely in less than twenty minutes. With less agglomeration, such as was obtained with 0.01 molar oxalic acid or 0.001 molar hydrochloric acid, a curve was obtained approaching the expected straight line. In none of the several experiments tried with these "surface-active" feldspars, however, was the theoretical curve for crushed materials attained. The effect of various dispersing agents, such as sodium pyrophosphate, sodium metasilicate, sodium carbonate, and aerosol, was determined, and in all cases a curve coinciding with that of the untreated material was obtained.

Particles as large as 3 or 4 microns were peptized. According to the usual notions of colloid chemistry,[23] such a phenomenon is limited to particles below approximately 0.5 micron. O'Meara, Norman, and Hammond[24] have found, however, that in flotation experiments weathered and unweathered feldspars behave differently with respect to ease of flotation.

The failure of particles under 3 to 4 microns to settle in pure water as fast as demanded by Stokes' law was observed for most but not all samples of type A feldspar. Type B feldspar and nepheline syenite, both of which hydrolyze at least to as great an extent as type A feldspar, did not show this effect. The coagulating effect of dilute magnesium sulfate, however, was shown on all the feldspars and on nepheline syenite but not on potter's flint.

Diatomaceous earth and very finely ground titania, neither of which shows base exchange, were flocculated by dilute magnesium sulfate solutions.

Several determinations of the particle size of type A feldspars were made with methyl alcohol as the suspending medium. The apparent particle-size distribution obtained was identical with that obtained when distilled water was used. Benzene was next tested as a suspending medium, but neither flint nor feldspar could be dispersed in it. Both settled out immediately no matter how much the mixture was stirred or shaken previously. Other nonpolar liquids, such as petroleum ether, dimethyl ether, carbon tetrachloride, and amyl acetate, yielded results similar to benzene. Acetone, which is intermediate in polarity between benzene and water, flocculated feldspar but allowed flint to settle according to the normal rate. At least one practical conclusion which may be drawn from these experiments is that great care must be taken in the choice of a suspending medium for particle-size studies as well as in the selection of any electrolyte that may be used. In cases where the degree of dispersion is doubtful, the use of logarithmic-probability plots to examine the data is extremely valuable, at least for ground substances.

(5) Hydrometer and Pipette Methods Compared

Two hydrometers were tested in this investigation. The first (No. 1 in Fig. 5) was the B type discussed in the A.S.T.M. Standard Method of Mechanical Analysis of Soils.[13] This type was also used by Thoreen,[25] who claimed that it yielded data in agreement with that obtained by pipette analysis. To check Thoreen's observation, the authors determined particle-size distributions for several flint samples by the hydrometer and Andreasen pipette methods. The particle-size and percentage data were calculated according to the formulas listed in section II. When these data were plotted on logarithmic-probability graph paper, the points obtained by the hydrometer method did not fall close to the straight line through the points obtained by the pipette method. It seemed advisable, therefore, to devise a calibration factor to correct the

[22] W. P. Kelley and H. Jenny, "Relation of Crystal Structure to Base Exchange and Its Bearing on Base Exchange in Soils," *Soil Sci.*, **41**, 367–82 (1936).

[23] E. A. Hauser, Colloidal Phenomena. McGraw-Hill Book Co., Inc., New York, 1939. 294 pp. *Ceram. Abs.* **18** [10] 283 (1939).

[24] R. G. O'Meara, J. E. Norman, and W. E. Hammond, "Froth Flotation and Agglomerate Tabling of Feldspars," *Bull. Amer. Ceram. Soc.*, **18** [8] 286–92 (1939).

[25] R. C. Thoreen, "Comments on the Hydrometer Method of Mechanical Analysis," *Public Roads*, **14**, 93–105 (1933).

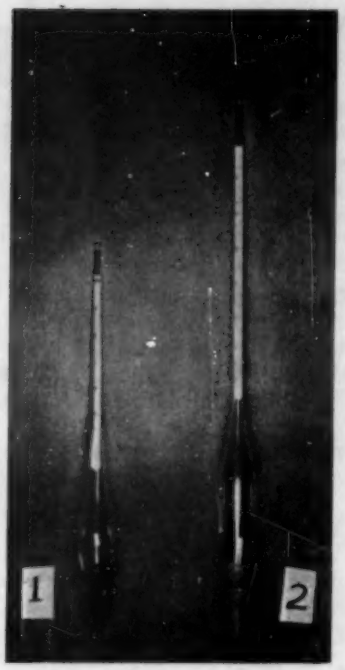

FIG. 5.—Hydrometers used in tests: No. 1, type B hydrometer discussed in A.S.T.M. standard test D422–39; No. 2, designed at Massachusetts Institute of Technology.

hydrometer values. Trial and error calculations showed that if formula (3)

$$\% = 100(R_s - 1)\left(\frac{D_1}{D_1 - D_2}\right)\frac{V}{W} \qquad (3)$$

be multiplied by the factor 0.794, values could be obtained that were in agreement with the pipette method. The validity of this procedure was tested by applying it to another sample and also to the same sample run at 20° C. Agreement between hydrometer and pipette values was obtained in both cases.

The other hydrometer (No. 2 in Fig. 5) was designed at the Soil Mechanics Laboratory, Massachusetts Institute of Technology. It differs from the A.S.T.M. B type in that the bulb is somewhat longer and has a cylindrical section between the sloping surfaces. A plot of the data obtained for a specific sample of flint again showed extreme deviation from the results obtained by pipette analysis. A calibration factor of 0.863 was calculated for this hydrometer and was tested by applying it to four different flints, one feldspar, and one zircon. Agreement between the hydrometer and pipette values was obtained in each case. One test was also made on flint at 20° and another on flint at a concentration of 25 gm. per liter. Good agreement again was obtained with the values from the pipette method, indicating that the correction factor can be used with confidence at least under these conditions of test. Because hydrometer No. 2 seems to be the more widely used at the present time, Fig. 1, which correlates hydrometer readings with distance of fall of particles for the M.I.T. hydrometer, is also included. The safest practice, however, would seem to be to calculate these distances versus specific gravity readings for each individual hydrometer.[26] All hydrometers, if they are to be used for discriminating tests, should obviously be calibrated according to the foregoing suggested method.

Using the correction factor, the hydrometer method was found to be nearly as accurate as the pipette method. The use of the hydrometer method in routine tests for particle-size distribution is therefore indicated. For plant control tests, it is proposed that two points be obtained by the hydrometer method and from them a log-probability plot be made. For example, readings may be taken at 5 and 60 minutes, corresponding to grain diameters of about 25 and 7 microns. Several samples may be run simultaneously with the starting times staggered one minute apart, which should permit accurate particle-size control in a minimum of operating time.

IV. Conclusions

The following conclusions may be drawn from the experimental results reported in this paper.

(1) The Andreasen pipette method is satisfactory for the laboratory determination of particle-size distribution of flints and feldspars in the subsieve range of 1 to 50 microns.

(2) For plant control of particle-size distribution in the subsieve range, the hydrometer method is adequate.

(3) The plotting of particle-size data on logarithmic-probability graph paper is a satisfactory procedure for the representation of particle-size distribution of ground materials. Specific surface (sq. cm. per gm.) values are easily calculated from such plots and are useful for comparing the fineness of different samples.

(4) Sieve data have no value in comparing materials as fine as the nonplastics generally used in whiteware manufacture. Such materials, however, may be expediently controlled by means of sedimentation analyses.

(5) Some samples of feldspar are peptizable in the particle-size range below 5 microns. All samples of the feldspar were found to be surface-active but none of the flints showed this property.

(6) Nonpolar liquids are not suitable suspending media for sedimentation analyses. The sedimentation velocities of very fine powders and surface-active powders are also greatly affected in aqueous media by many electrolytes.

RESEARCH LABORATORIES
WESTINGHOUSE ELECTRIC AND MANUFACTURING COMPANY
EAST PITTSBURGH, PENNSYLVANIA

[26] H. E. Schweyer, "Particle-Size Studies," *Ind. Eng. Chem., Anal. Ed.*, **14**, 622–32 (1942); *Ceram. Abs.*, **21** [11] 245 (1942).

BRUCITE MAGNESIA*

By M. F. Goudge

Abstract

A discussion of the occurrence of brucite in limestone, the method of extracting it in the form of magnesia, and uses for which this particular type of magnesia is best suited is presented with emphasis on the possibilities of brucite magnesia in the ceramic industry.

I. Introduction

A new type of magnesia possessing unusual physical and chemical properties is being produced from brucitic limestone near Wakefield, Quebec, and is being used for making basic refractories for the copper, steel, nickel, and other metallurgical industries, for making a special grade of paper needed in munitions, for fertilizers, and for various other ceramic and chemical uses. The magnesia is particularly suitable for the manufacture of magnesium metal by direct chlorination, and, because of its purity and the ease with which its activity may be controlled by a small amount of additional processing, it has interesting potentialities for a variety of other uses.

The plant producing this magnesia is owned and operated by the Aluminum Company of Canada and is situated among a number of deposits of brucitic limestone. The use of diamond drilling has indicated the existence of millions of tons of this material. This plant has a rated daily capacity of 50 tons of magnesia and 100 tons of by-product hydrated lime.

The process used was developed in the laboratories of the Bureau of Mines at Ottawa after the discovery of the brucite near Rutherglen, Ontario, by the Bureau in 1937 and its subsequent discoveries at Bryson and Wakefield in the province of Quebec.[1]

II. Description of Brucitic Limestone

Brucitic limestone, referred to in mineralogy as predazzite and pencatite, consists of granules of magnesium hydroxide, or brucite, disseminated through a matrix of highly crystalline limestone. The granules of brucite are rudely spherical, composed of scales arranged concentrically, about $1^1/_2$ to $2^1/_2$ mm. in diameter, and of a high degree of purity.

Freshly broken brucitic limestone looks much like ordinary crystalline limestone, and this similarity explains why the true nature of the deposits was so long unrecognized even though some of the deposits were worked at various times to obtain building stone, road metal, and stone for making lime.

The brucite content of the deposits in the Wakefield district is about 29% by weight of the rock, which is equivalent to 20% of magnesia. The actual magnesia content is slightly higher than this figure because of small amounts of dolomite and serpentine that are also present.

Analyses of brucite limestone closely correspond with those of dolomite, and there seems to be little room for doubt that the deposits originated from huge blocks of dolomite caught up in the flow of igneous rock that surrounds them. Conditions of temperature and pressure could have been such that only the magnesium carbonate component of the dolomite was calcined, leaving the calcium carbonate component undissociated. The magnesia was subsequently altered to brucite. A feature of the Canadian brucitic limestone deposits is that, because of their greater resistance to erosion than that of the syenite and granite surrounding them, they generally form prominent hills, which is advantageous from the quarrying standpoint.

III. Processing of Brucitic Limestone

The process developed in the Bureau of Mines for the production of magnesia in granular form from brucitic limestone involves (1) calcining brucitic limestone under carefully controlled conditions, (2) hydrating the calcine under carefully controlled conditions with only sufficient water to convert the lime to a dry hydrated powder and to leave the calcined brucite unhydrated and in granular form, (3) separating the hydrated lime from the granules of magnesia in an air separator, (4) washing the granules in such a way that they will not become hydrated, and (5) drying the granules quickly to avoid their hydration.

The yield and purity of the product depend on the technical skill and degree of control maintained from the quarrying of the rock to the final drying. Reasonably pure brucitic limestone is essential in order to obtain a high yield and a pure product simultaneously, and quarry operations must be conducted with this fact in mind. Some large bodies of brucitic limestone are sufficiently free from impurities to be utilized without cobbing, but in other parts of the deposits veins and irregular patches of yellow, brown, and green serpentine may occur in what would otherwise be high-grade rock.

(1) Calcination and Hydration

Calcination is done in rotary kilns under close temperature control. Brucitic limestone will calcine more

* Presented at the Forty-Fifth Annual Meeting, The American Ceramic Society, Pittsburgh, Pa., April 21, 1943 (Materials and Equipment Division). Received April 21, 1943; revised paper received October 8, 1943.

Presentation and publication authorized by the Director, Mines and Geology Branch, Department of Mines and Resources, Ottawa, Ontario, Canada.

[1] M. F. Goudge, "Preliminary Report on Brucite Deposits in Ontario and Quebec and Their Commercial Possibilities," *Can. Dept. Mines, Bur. Mines, Mines & Geol. Branch, Dept. Mines & Resources, Memorandum Series*, No. 75 (Dec., 1939); *Ceram. Abs.*, 19 [11] 267 (1940).

rapidly and at a lower temperature than will ordinary limestone. For a brucitic limestone having a calcite matrix, the maximum temperature should not exceed 2150°F. for any considerable length of time in order to obtain a product low in lime. The calcining temperature also has a marked effect on the chemical activity of the granules. If the Wakefield brucitic limestone is subjected to a temperature in excess of 2250°F. for more than one-half hour, the magnesia recovered is relatively inactive and takes up water of hydration only very slowly. When magnesia is produced for refractory uses, this slow hydration may be an advantage and the highest temperature consistent with a low-lime product may be used, yielding a high kiln output. When a magnesia with a high degree of activity is desired, however, the rock must be calcined at the lowest temperature consistent with complete calcination within a reasonable time. This temperature may be as low as 1800°F.

The differential hydration of the calcine is accomplished in a continuous hydrator similar to those used in the lime industry. Just sufficient water to convert all of the lime to a dry hydrate is added. It is essential that the hydration of the magnesia granules be prevented while that of the lime is facilitated; the magnesia granules otherwise will become powdered, disintegrate, and have a low yield. Because high temperature combined with moisture is ideal for the hydration of magnesia, the temperature of the hydrating lime must be kept as low as is consistent with the completion of the reaction within a reasonable period of time and the material must be thoroughly agitated while the hydration of the lime is in progress.

(2) Separation of Lime and Magnesia

The hydrated lime is separated from the magnesia granules in an air separator of conventional design. The feed to the separator is passed through a 4-mesh screen to remove any pieces of core, large fragments of serpentine, or other impurities. The lime discharged from the separator is ready for bagging and marketing as hydrated lime. The oversize material from the air separator, consisting of all the granules, some hydrated lime, and some small lumps of unslaked lime, is passed to a washing unit.

(3) Washing and Drying Magnesia Granules

To insure the slaking of any lumps of quicklime that may be mixed with the granules, the oversize material from the air separator is fed to a large rotating cylinder where sufficient water is added to make a thin slurry and to permit the quicklime to slake to a milk of lime. The lime slurry containing the granules is pumped to a classifier where, in an excess of cold water, the lime is removed, and the granular product is discharged to a vibrating screen equipped with water sprays. The product at this stage consists of granules of magnesia mixed with tiny rounded grains of calcined serpentine, which was originally present in the rock with the the brucite. These serpentine granules consist chiefly of minus 35-mesh screen, whereas most of the brucite is plus 35-mesh. Separation of the magnesia and the serpentine is made on the vibrating screen, which may be 35-mesh or finer, if the rock is pure, or 28-mesh, if the rock contains considerable serpentine. Material that passes the washing screen consists partly of brucite magnesia and is stored in a tailings pond for future utilization. The oversize material from the washing screen is dewatered to remove as much free moisture as possible before it goes to the drier.

The granules must be dried without allowing an undue amount of hydration to take place. When they are ready for drying, properly processed granules contain not more than 2% of water of hydration distinct from the surface moisture. Unless drying is rapid, however, the granules are apt to become hydrated to the extent of 6 or 8% in this part of the operation alone. A rotary steam-heated drier gives a dry product with little additional hydration if it is operated at low capacity, but under a heavy load the product may contain from 5 to 7% of water of hydration. Flash drying, using the heat in the gases leaving the kiln, appears to be a suitable method to dry the granules economically and at the same time to prevent hydration.

IV. Characteristics of Granular Brucite Magnesia

The finished product consists essentially of hard, rounded granules of magnesia ranging in size from 8- to 35-mesh and possessing a high degree of chemical purity. As normally recovered, the magnesia granules possess only a moderate degree of chemical activity because of the high temperature at which the brucitic limestone has been calcined. After long periods of storage the granules will take up only a small percentage of water. They may be made as reactive as desired, however, by hydration under conditions of heat and moisture and by recalcination at a temperature under 1000°F.

When an active magnesia is required, the original calcination should be at the lowest temperature consistent with thorough calcination of the calcite matrix. The granules, instead of being dried, are hydrated with the aid of steam. Complete hydration (to the state of brucite) may be effected in less than one hour. This degree of hydration, however, is rarely necessary.

V. Uses of Brucite Magnesia

The greater part of the brucite magnesia produced at the present time is sold to Canadian Refractories, Ltd., where, after being dead-burned, the granules are used for the manufacture of basic refractories of special grade. The dead-burned granules possess certain physical properties that make them highly desirable for producing fired and chemically bonded basic brick. These brick are currently being used in reverberatory and open-hearth furnaces, in converters, and in electric furnaces in the copper, nickel, steel, and other metallurgical industries. As a basic brick, they possess remarkable refractory and spalling-resistant properties, particularly in furnaces that are operating at temperatures higher than those normally used. An initial trial of brucite brick in the roof of a large reverberatory furnace operating under unusual conditions has given satisfactory results.

Dead-burned brucite magnesia is also giving satisfactory service as a chemically bonded hearth ramming mix, particularly in electric furnaces.

Pulverized brucite magnesia is being shipped abroad for making a special grade of paper used in munitions. In the pulverized state, it is also being used in chemical fertilizers. After being recalcined at 2700°F. and pulverized, the magnesia is as useful as fused periclase for a refractory powder to seal carbon resistance furnaces for firing certain ceramic materials at high temperatures and under reducing conditions.

Experiments are now under way in the laboratories of the Industrial Minerals Division of the Bureau of Mines to develop the use of brucite magnesia as a substitute for talc in special porcelain bodies that possess a low coefficient of thermal expansion. Experiments are also being conducted in these laboratories to ascertain its usefulness for enriching steatite electrical insulation bodies in magnesia. These investigations were started only recently and results are not yet conclusive.

Because of its purity, the brucite magnesia also appears to be suitable for use in tamped linings of crucibles for induction furnaces and for other refractory linings requiring a basic material.

INDUSTRIAL MINERALS DIVISION
BUREAU OF MINES
OTTAWA, CANADA

CHANGES OF PROPERTIES OF GLASS RESULTING FROM CHANGES OF COMPOSITION*

BY MAURICE L. HUGGINS AND KUAN-HAN SUN

ABSTRACT

Equations are given for the calculation of changes of density, refractive index, and other optical constants produced by the addition of a known relative weight of a given component to a base glass. Corresponding equations for the substitution of one component for another are also given. Values are computed and listed for the initial fractional rate of change of refractive index (n_D) when various components are added to (*a*) pure SiO_2 and (*b*) a sodium silicate glass containing 50% of Na_2O by weight.

I. Introduction

The authors, in a recent paper,[1] have given methods for the calculation of the density and various optical properties of a glass from its composition, expressed in percentage by weight. Investigators in the field of glass technology are also interested in the effect on the properties of a glass of the addition or substitution of a certain component. It is the purpose of this paper to present a general method for the calculation of the changes in density and optical properties of a glass when a small amount of a given oxide is added to a glass of known composition or properties or is substituted for another component already in the glass.

II. Derivation of Equations

Let f^0_M represent the weight fraction of any component M_mO_n in the base glass; let f'_A represent the weight of the added component (A_mO_n) divided by the weight of base glass to which it is added; and let f_M represent the weight fraction of any component in the glass after the addition. From these definitions, equations (1) through (3) are obtained.

$$\sum f^0_M = 1 \tag{1}$$

$$\sum f_M = 1 \tag{2}$$

$$f_A = \frac{f'_A}{1 + f'_A} \tag{3}$$

For all components except A_mO_n, equation (4) will apply.

$$f_M = \frac{f^0_M}{1 + f'_A} \tag{4}$$

In the paper to which reference has already been made,[1] the relationships represented by equations (5) through (10) are given.

$$v \equiv \frac{1}{\rho} = \sum f_M v_M \tag{5}$$

$$r_D \equiv \frac{n_D - 1}{\rho} = \sum f_M r_{M,D} \tag{6}$$

$$\mu_D \equiv n_D - 1 = \frac{r_D}{v} = \frac{\sum f_M r_{M,D}}{\sum f_M v_M} \tag{7}$$

$$n_{\lambda_1} - n_{\lambda_2} = \frac{\sum f_M r_{M,\lambda_1-\lambda_2}}{\sum f_M v_M} \tag{8}$$

$$p \equiv \frac{n_D - 1}{n_F - n_C} = \frac{\sum f_M r_{M,D}}{\sum f_M r_{M,F-C}} \tag{9}$$

$$\frac{n_{\lambda_1} - n_{\lambda_2}}{n_{\lambda_3} - n_{\lambda_4}} = \frac{\sum f_M r_{M,\lambda_1-\lambda_2}}{\sum f_M r_{M,\lambda_3-\lambda_4}} \tag{10}$$

* Presented at the Forty-Fifth Annual Meeting, The American Ceramic Society, Pittsburgh, Pa., April 20, 1943 (Glass Division). Received April 3, 1943.

Communication No. 918 from the Kodak Research Laboratories.

[1] M. L. Huggins and K.-H. Sun, "Calculation of Density and Optical Constants of a Glass from Its Composition in Weight Percentage," *Jour. Amer. Ceram. Soc.*, **26** [1] 4–11 (1943).

The density of the glass is denoted by ρ, and n_D, n_F, n_λ, etc., denote its index of refraction for the wave length indicated by the subscript; v (the specific volume), r_D (the specific refraction for the sodium D line), μ and ν are defined by the identity equations (denoted by $\equiv$) given; and v_M, $r_{M,D}$, $r_{M,F-C}$, $r_{M,\lambda_1-\lambda_2}$, and $r_{M,\lambda_3-\lambda_4}$ are constants characteristic of the components. Values of v_M, $r_{M,D}$, and $r_{M,F-C}$ for many components have been listed by Huggins and Sun.[1]

It should be noted that whereas the r_M constants are in general independent of the composition of the glass, four sets of v_M constants are required (for silicate glasses), each set being applicable to a limited composition range only.[2]

Equations (5) to (10), inclusive, are all of form (11).

$$\phi = \frac{\sum f_M \alpha_M}{\sum f_M \beta_M} \tag{11}$$

$$\phi = \sum f_M \alpha_M \tag{12}$$

(Equation (12), exemplified by equations (5) and (6), is a special case of equation (11) and is obtained from it by putting all β_M values equal to unity.)

The general equation (13) obviously represents the dependence on composition of each property (v, r, etc.) of the base glass.

$$\phi^0 = \frac{\sum f^0_M \alpha_M}{\sum f^0_M \beta_M} \tag{13}$$

$$\phi = \frac{f_A\alpha_A + \sum' f_M \alpha_M}{f_A\beta_A + \sum' f_M \beta_M} \tag{14}$$

Equation (14) is obtained after the addition of a component A_mO_n to this base glass, the primes signifying that no term for component A_mO_n is to be included in the summations. Substitution of equations (3) and (4) gives equation (15).

$$\phi = \frac{f'_A\alpha_A + \sum f^0_M \alpha_M}{f'_A\beta_A + \sum f^0_M \beta_M} \tag{15}$$

The change in the property is shown therefore in equation (16).

$$\phi - \phi^0 = \frac{f'_A(\alpha_A - \beta_A\phi^0)}{f'_A\beta_A + \sum f^0_M \beta_M} \tag{16}$$

For small values of f'_A, this relation simplifies to equation (17).

$$\phi - \phi^0 \approx \phi^0 f'_A\left[\frac{\alpha_A}{\sum f^0_M \alpha_M} - \frac{\beta_A}{\sum f^0_M \beta_M}\right] \tag{17}$$

The fractional rate of change of ϕ with f'_A (at the limit, $f'_A = 0$) is thus given by equation (18).

$$\frac{1}{\phi^0}\left(\frac{d\phi}{df'_A}\right)_{f'_A=0} = \frac{\alpha_A}{\sum f^0_M \alpha_M} - \frac{\beta_A}{\sum f^0_M \beta_M} \tag{18}$$

For functions (e.g., v or r_D) represented by equations of the form of equation (12) (putting $\beta_A = \beta_M = 1$), equations (19), (20), and (21) may be deduced.

$$\phi - \phi^0 = \left(\frac{f'_A}{1 + f'_A}\right)(\alpha_A - \phi^0) \tag{19}$$

$$\approx f'_A(\alpha_A - \phi^0) \text{ for small } f'_A \tag{20}$$

$$\frac{1}{\phi^0}\left(\frac{d\phi}{df'_A}\right)_{f'_A=0} = \left(\frac{\alpha_A}{\phi^0} - 1\right) \tag{21}$$

If a given weight of one component, A_mO_n, is substituted for the same weight of another, B_mO_n, in the base glass, similar reasoning gives equations (22) and (23) in place of equations (16) and (18).

$$\phi - \phi^0 = \frac{f'_A[(\alpha_A - \alpha_B) - (\beta_A - \beta_B)\phi^0]}{f'_A(\beta_A - \beta_B) + \sum f^0_M \beta_M} \tag{22}$$

$$\frac{1}{\phi^0}\left(\frac{d\phi}{df'_A}\right)_{f'_A=0} = \frac{\alpha_A - \alpha_B}{\sum f^0_M \alpha_M} - \frac{\beta_A - \beta_B}{\sum f^0_M \beta_M} \tag{23}$$

The summations, $\sum f^0_M \beta_M$ and $\sum f^0_M \alpha_M$, in equations (15) to (23) can be replaced (see equations (5) and (6)) by v^0, r^0_D, $r^0_F - r^0_C$, etc., properties of the base glass. The composition of that glass need not be known.

An added (or subtracted) component, A_mO_n (or B_mO_n), may of course be the same as one of the components in the base glass. In that case, f'_A is obviously the *additional* fractional weight of added oxide.

III. Example: Change of Refractive Index

As an illustration of the use of the foregoing relationships, consideration may be given to the effect on the refractive index, n_D, of the addition of f'_A gram (or other weight unit) of an oxide, A_mO_n, to one gram (or other weight unit) of a base glass having a density ρ^0 and an index of refraction n^0_D. For this case (cf. equations (5), (7), and (11)), equations (24) through (27) apply.

$$\phi \equiv n_D - 1 \tag{24}$$

$$\alpha_M \equiv r_{M,D} \text{ and } \alpha_A \equiv r_{A,D} \tag{25}$$

$$\beta_M \equiv v_M \text{ and } \beta_A \equiv v_A \tag{26}$$

$$\sum f^0_M \beta_M = v^0 \equiv \frac{1}{\rho^0} \tag{27}$$

Substitution into equation (16) yields equation (28).

$$n_D - n^0_D = \frac{f'_A[r_{A,D} - v_A(n^0_D - 1)]}{f'_A v_A + \frac{1}{\rho^0}} \tag{28}$$

Values of $r_{A,D}$ and v_A for many oxide components are available (listed as $r_{M,D}$ and v_M by Huggins and

[1] M. L. Huggins, "Density of Silicate Glasses as Function of Composition," *Jour. Optical Soc. Amer.*, **30** [9] 420–30 (1940); *Ceram. Abs.*, **20** [2] 41 (1941).
See also reference 1.

TABLE I

CHANGE OF REFRACTIVE INDEX WITH COMPOSITION

Added component	$\frac{1}{\mu^0_D}\left(\frac{d\mu_D}{df'_A}\right)_{f'_A=0}$ Base glass: SiO_2	Base glass: sodium silicate ($f^0_{Na} = 0.5000$)	Added component	$\frac{1}{\mu^0_D}\left(\frac{d\mu_D}{df'_A}\right)_{f'_A=0}$ Base glass: SiO_2	Base glass: sodium silicate ($f^0_{Na} = 0.5000$)
Li_2O	0.9041	0.3712	La_2O_3*	0.4939	0.3510
Na_2O	0.31292	0.00755	Pr_2O_3*	0.4994	0.3592
K_2O	0.2475	0.00567	Nd_2O_3*	0.4465	0.3036
Rb_2O	0.1209	−0.0215	Sm_2O_3*	0.4345	0.2997
Tl_2O	0.4727	0.4226	Gd_2O_3*	0.3509	0.2109
BeO	0.8689	0.2800	Er_2O_3*	0.3572	0.2269
MgO	0.4435	0.0241	Fe_2O_3	1.4952	1.2255
CaO	0.6786	0.3907	Bi_2O_3	0.5596	0.4665
ZnO	0.4224	0.2190	SiO_2	0	−0.00753
SrO	0.4451	0.2782	TiO_2	1.1146	0.7366
CdO	0.3990	0.2721	ZrO_2	0.7171	0.4691
BaO	0.3908	0.2773	CeO_2*	0.5369	0.3565
PbO	0.4331	0.3604	ThO_2*	0.3672	0.2460
B_2O_3 (B′)		−0.4435	V_2O_5*	0.7839 (?)	0.2923 (?)
B_2O_3 (B″)	0.0106		Cb_2O_5*	0.8224	0.5402
Al_2O_3	0.3310	−0.1724	Ta_2O_5	0.4238	0.2452
Ga_2O_3*	0.3579	0.0881	MoO_3*	0.4730	0.1148
Yt_2O_3*	0.5065	0.2872	WO_3*	0.4351	0.2285
In_2O_3*	0.4877	0.3241	UO_3*	0.3757	0.2090

* Values for these oxides were computed with the aid of density data kindly furnished by J. C. Young of the National Bureau of Standards, Washington, D. C.

Sun[1]). These, with the known magnitudes of f'_A, n^0_D, and ρ^0, suffice for the calculation of $n_D - n^0_D$ (and so of n_D) by means of equation (28). (Care must be taken to use v_A values appropriate to the silica concentration present in the glass. If this changes during the addition of A_mO_n, from a range for which one set of v_A values is characteristic to another range, corresponding to another set of v_A values, the calculations are somewhat more complicated than those described here.)

Comparison of the relative effect on n_D of different oxides is most conveniently made with the aid of equation (18). Making appropriate substitutions, the limiting fractional rate of change of μ_D with f'_A is found to be as given by equation (29).

$$\frac{1}{\mu^0_D}\left(\frac{d\mu_D}{df'_A}\right)_{f'_A=0} = \frac{1}{n^0_D - 1}\left(\frac{dn_D}{df'_A}\right)_{f'_A=0} = \rho^0\left(\frac{r_{A,D}}{n^0_D - 1} - v_A\right) \quad (29)$$

Values of $\frac{1}{\mu^0_D}\left(\frac{d\mu_D}{df'_A}\right)_{f'_A=0}$ for the addition of various components to two base glasses (SiO_2 and a sodium silicate glass having $f^0_{Na} = 0.5000$) are collected in Table I. For other sodium silicate glasses intermediate in composition between these two, the initial fractional rate of change of μ_D with f'_A for each component should be intermediate between the two values given.

For relatively small additions, the change in refractive index ($n_D - n^0_D = \mu_D - \mu^0_D$) is obtained from the appropriate value of $\frac{1}{\mu^0_D}\left(\frac{d\mu_D}{df'_A}\right)_{f'_A=0}$ merely by multiplying by the μ^0_D ($= n^0_D - 1$) value for the base glass and by the value of f'_A.

EASTMAN KODAK COMPANY
ROCHESTER, NEW YORK

GLASS PROPERTIES AND THE PERIODIC TABLE*

By Maurice L. Huggins and Kuan-Han Sun

Abstract

Graphs are presented showing the variation with atomic number and with group of the periodic table of certain constants entering into the calculation of densities, refractive indices, and dispersions of glasses.

I. Introduction

The purpose of this paper is to present graphs showing the variation of certain constants, characteristic of oxide components of glasses, with the position in the periodic table of the more metallic (i.e., the nonoxygen) element of the component.

In each graph, the magnitude of the constant is plotted against atomic number. Points for oxides of elements in the same subgroup are connected by lines; broken lines are used if consecutive points do not represent consecutive elements in the subgroup. The two classes of subgroups, A and B, are plotted separately but are placed side by side to facilitate comparison.

These graphs show clearly the relative effect of different components on certain properties of glasses, whether simple or complex in composition. They should, therefore, prove useful technologically. Rough values may also be obtained for additional components by extrapolation and interpolation.

The accuracy of the constants plotted varies greatly, depending on the extent and accuracy of the experimental data from which they were computed. Some of the irregularities in the curves are doubtless attributable to inaccurate or insufficient data; others, however, are certainly a result of the dependence of the property concerned on some quantity (e.g., coordination number of the nonoxygen element) which does not vary smoothly and continuously with atomic number.

Space will not be taken here to discuss the theoretical implications of the regularities and irregularities shown. The authors hope to deal with this matter at a later date.

II. Density

The constants, c_M, plotted in Fig. 1, enter into the calculation of the density, ρ, of a silicate glass by means of equation (1).[1]

$$\rho = \frac{1}{\left(k + b_{Si} + \sum c_M N_M\right)\sum\left(n_M f_M / W_M\right)} \qquad (1)$$

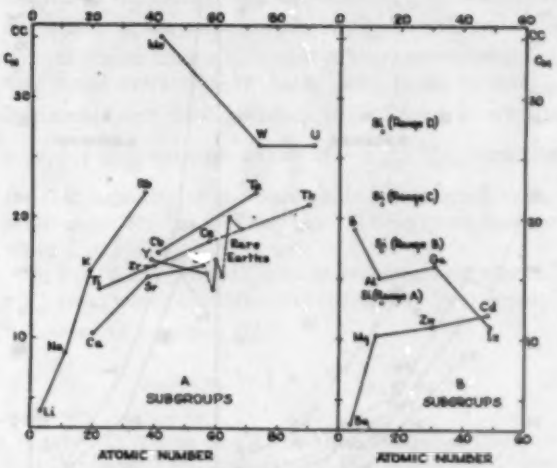

Fig. 1.—Volume constants, c_M.

k = a small constant, whose magnitude depends on annealing technique.

b_{Si} and c_{Si} (= c_M for component SiO_2) = constants having different values for different ranges of N_{Si}.

N_M = number of atoms of element M per atom of oxygen in the glass.

n_M = subscript of O in formula of a component, M_mO_n.

f_M = weight fraction of that component.

W_M = its molecular weight.

The summations are over all the components present in the glass. With regard to the computation of N_M, see references 1 or 2.

Most of the c_M values plotted are those listed previously by the authors.[2] A few additional values have been computed with the aid of density data furnished by Young.*

As has previously been shown,[2(a)] the density may also be computed from "specific volume constants" by means of the simpler equation, (2).

$$\rho = \frac{1}{\sum v_M f_M} \qquad (2)$$

---

* Presented at the Forty-Fifth Annual Meeting, The American Ceramic Society, Pittsburgh, Pa., April 20, 1943 (Glass Division). Received April 16, 1943.

Communication No. 926 from the Kodak Research Laboratories.

[1] M. L. Huggins, "Density of Silicate Glasses as Function of Composition," *Jour. Optical Soc. Amer.*, **30** [9] 420–30 (1940); *Ceram. Abs.*, **20** [2] 41 (1941).

[2] (*a*) M. L. Huggins and K.-H. Sun, "Calculation of Density and Optical Constants of a Glass from Its Composition in Weight Percentage," *Jour. Amer. Ceram. Soc.*, **26** [1] 4–11 (1943).

(*b*) See also reference 1.

* J. C. Young, National Bureau of Standards, Washington, D. C., to whom the authors wish to express their indebtedness. Young has also supplied some of the data on which Figs. 2, 3, 10, and 11 are based.

Different sets of v_M constants are required, however, for different ranges of N_{Si} values. Two of the sets (for use with glasses which are very low and very high, respectively, in silica content) are plotted in Figs. 2 and 3.

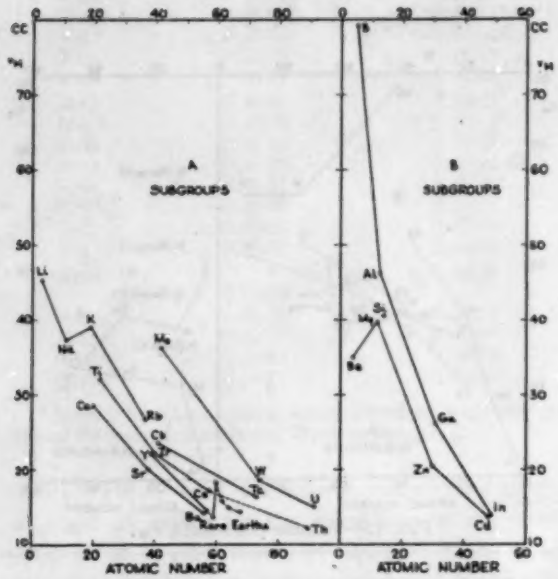

FIG. 2.—Specific volume constants, v_M, for composition range A (low silica content).

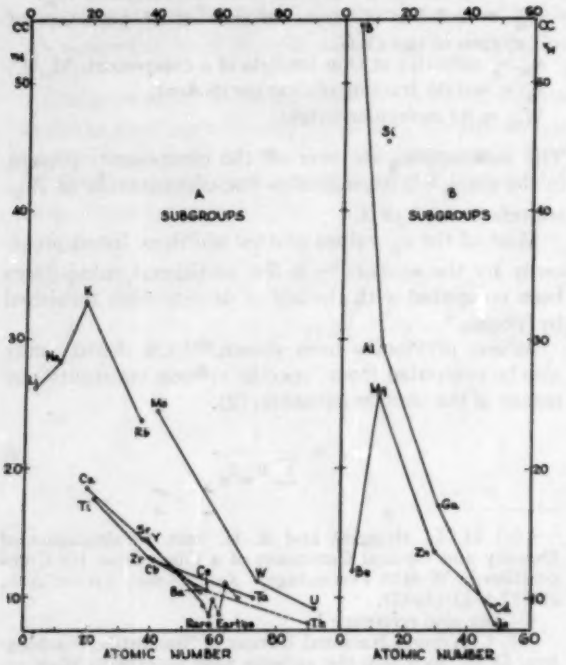

FIG. 3.—Specific volume constants, v_M, for composition range D (high silica content).

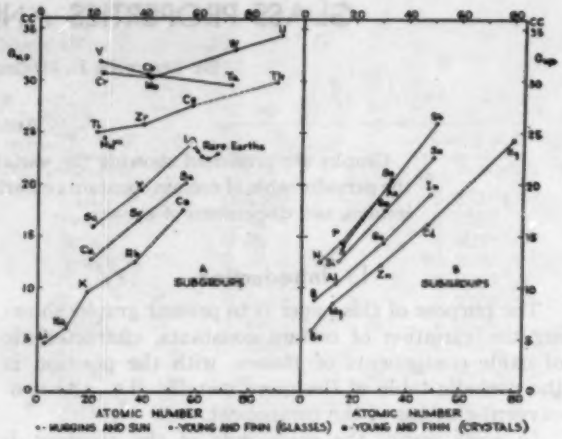

FIG. 4.—Refraction constants, $a_{M,D}$

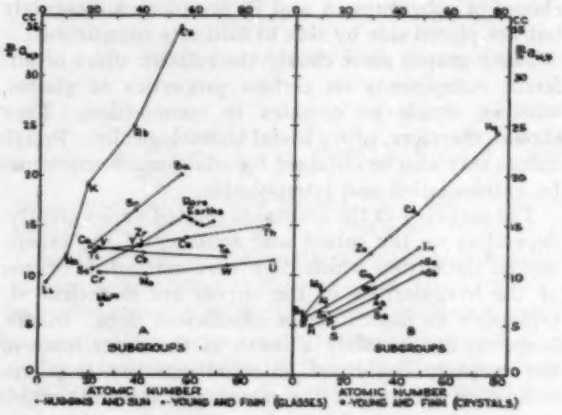

FIG. 5.—Refractions for an amount of pure oxide containing one gram-atom of oxygen.

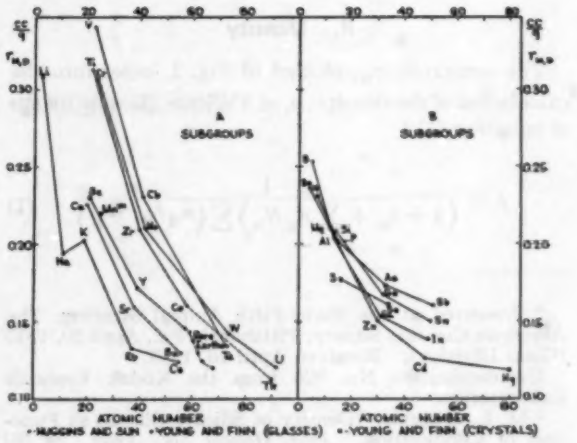

FIG. 6.—Specific refraction constants, $r_{M,D}$

III. Refractive Index

The constants, $a_{M,D}$, plotted in Fig. 4 are those entering into the calculation of the refractive index by means of equations (3) and (4).[3]

$$\mu_D \equiv n_D - 1 = \frac{\sum a_{M,D} N_M}{V_O} \qquad (3)$$

[3] M. L. Huggins, "Refractive Index of Silicate Glasses as Function of Composition," *Jour. Optical Soc. Amer.*, **30** [10] 495–504 (1940); *Ceram. Abs.*, **20** [2] 41–42 (1941).

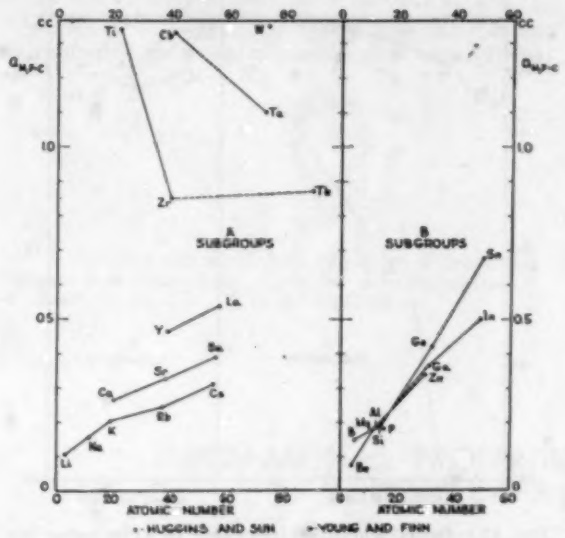

FIG. 7.—Dispersion constants, $a_{M,F-C}$.

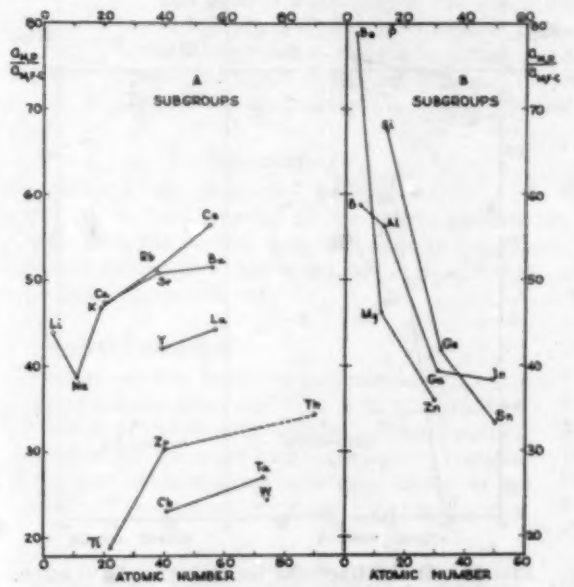

FIG. 8.—Abbe values for pure oxides.

$$V_O = \frac{1}{\rho \sum (n_M f_M / W_M)} \qquad (4)$$

The values plotted have been listed previously[2,3] except for those (■) deduced entirely from crystal data, which were computed from "specific refraction constants" (see the second paragraph following) published by Young and Finn.[4]

On the assumption (which is at least a good approximation to the truth) that the same $a_{M,D}$ constants are applicable to the pure oxides, M_mO_n, as well as to the silicate glasses from which most of them were computed, the molal refraction of each pure oxide is $ma_{M,D}$. For some theoretical purposes, it is of more interest to compute and compare values of $\frac{m}{n}a_{M,D}$, the refraction for that quantity of the pure oxide which contains one gram-atom (16 gm.) of oxygen. These quantities are plotted in Fig. 5.

In Fig. 6 are plotted "specific refraction constants," $r_{M,D}$, from which the refractive index may be computed by means of equation (5).[4]

$$\mu_D \equiv n_D - 1 = \rho \sum r_{M,D} f_M \qquad (5)$$

[4] (*a*) J. C. Young and A. N. Finn, "Effect of Composition and Other Factors on Specific Refraction and Dispersion of Glasses," *Jour. Research Nat. Bur. Standards*, **25** [6] 759–82 (1940); R. P. 1352; *Ceram. Abs.*, **20** [4] 88 (1941).

(*b*) J. C. Young and A. N. Finn, "Comparison of Two Recent Studies on Refraction and Dispersion of Glasses," *Jour. Optical Soc. Amer.*, **31** [5] 383–84 (1941); *Ceram. Abs.*, **20** [8] 191 (1941).

(*c*) See also reference 2(*a*).

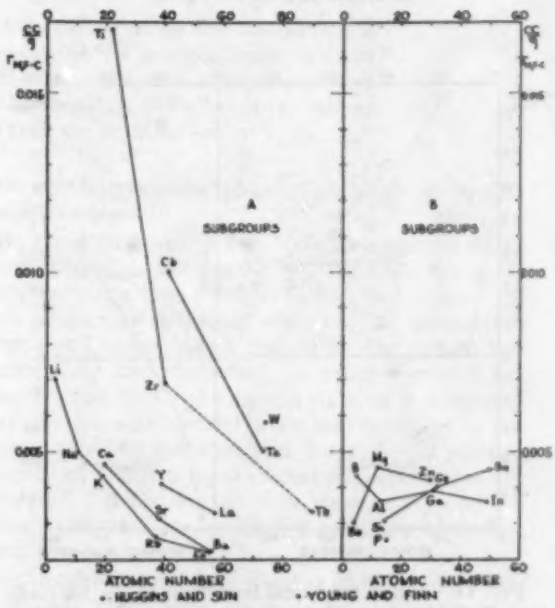

FIG. 9.—Specific dispersion constants, $r_{M,F-C}$.

IV. Dispersion

Figure 7 shows the dispersion constants,[5] $a_{M,F-C}$, from which the dispersion of a glass may be computed, using equation (6).

$$n_F - n_C = \frac{\sum a_{M,F-C} N_M}{V_O} \qquad (6)$$

The dependence on atomic number of the ratio, $a_{M,D}/a_{M,F-C}$, is shown in Fig. 8. These ratios are Abbe values, $\left(\nu \equiv \frac{n_D - 1}{n_F - n_C}\right)$.

[5] (*a*) M. L. Huggins, "Dispersion of Silicate Glasses as Function of Composition," *Jour. Optical Soc. Amer.*, **30** [11] 514–18 (1940); *Ceram. Abs.*, **20** [4] 88 (1941).
(*b*) M. L. Huggins, K.-H. Sun, and D. O. Davis, "Dispersion of Silicate Glasses as Function of Composition, II," *Jour. Optical Soc. Amer.*, **32** [12] 635–50 (1942); *Ceram. Abs.*, **22** [2] 30 (1943).

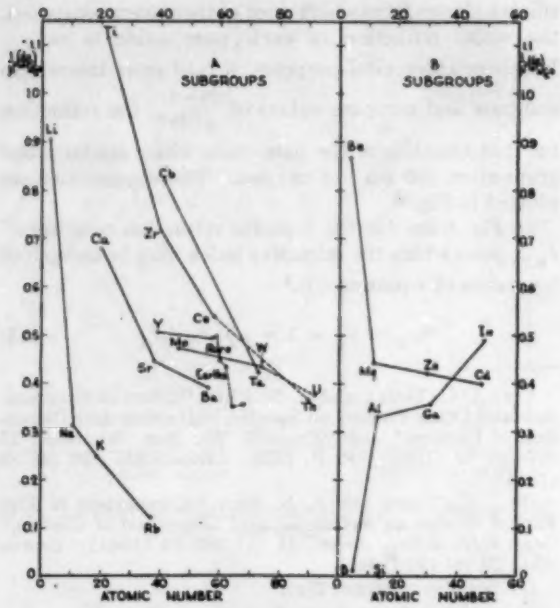

FIG. 10.—Initial fractional increment in μ_D, for addition of oxides to pure SiO_2 glass.

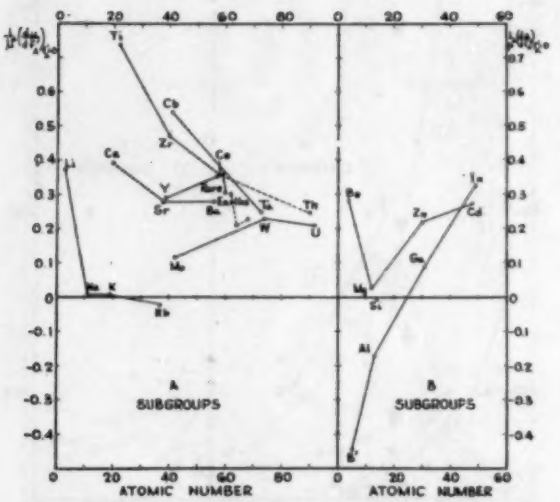

FIG. 11.—Initial fractional increment in μ_D, for addition of oxides to a glass of composition (by weight), Na_2O 50%, SiO_2 50%.

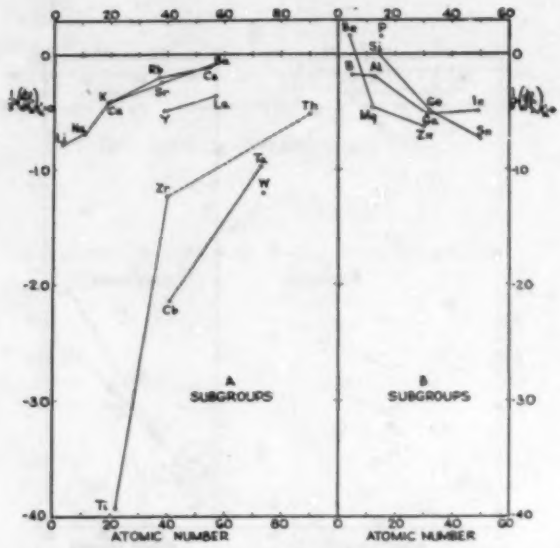

FIG. 12.—Initial fractional increment in Abbe value, for addition of oxides to pure SiO_2 glass.

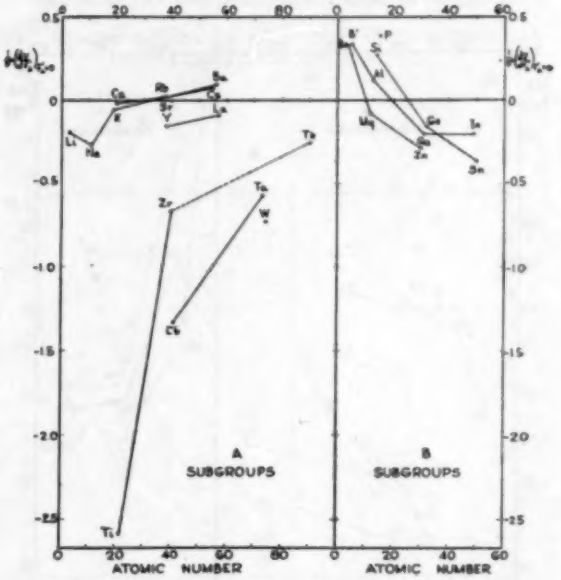

FIG. 13.—Initial fractional increment in Abbe value, for addition of oxides to a glass of composition (by weight), Na_2O 50%, SiO_2 50%.

for the pure oxides, assuming the $a_{M,D}$ and $a_{M,F-C}$ values computed for silicate glasses to be applicable also to these oxides.

Figure 9 shows the "specific dispersion constants," $r_{M,F-C}$, related to the dispersion of a glass by equation (7).[4]

$$n_F - n_C = \rho \sum r_{M,F-C} f_M \qquad (7)$$

V. Initial Fractional Increments

Figures 10 through 13 show the initial fractional increment in μ and in v, for addition of a component A_mO_n, to a base glass consisting of pure SiO_2 (Figs. 10 and 12) and a sodium silicate glass, in which $f_{Na} = f_{Si} = 1/2$ (Figs. 11 and 13). The quantities plotted have been computed by means of equations (8) and (9).[4]

$$\frac{1}{\mu^0_D}\left(\frac{d\mu_D}{df'_A}\right)_{f'_A=0} = \rho^0\left(\frac{r_{A,D}}{\mu^0_D} - v_A\right) \qquad (8)$$

$$\frac{1}{v^0}\left(\frac{dv}{df'_A}\right)_{f'_A=0} = \frac{r_{A,D}}{r^0_D} - \frac{r_{A,F-C}}{r^0_{F-C}} \qquad (9)$$

[4] M. L. Huggins and K.-H. Sun, "Changes of Properties of Glass Resulting from Changes of Composition," *Jour. Amer. Ceram. Soc.*, **27** [1] 10–12 (1943).

f'_A = weight of added oxide, A_mO_n, divided by weight of base glass to which it is added.
μ^0_D, ρ^0, r^0_D, r^0_{F-C}, and v^0 = properties of base glass.
$r_{A,D}$, v_A, and $r_{A,F-C}$ = characteristic glass constants for component A_mO_n.

The initial fractional increment in v may be computed[4] from equation (10).

$$\frac{1}{v^0}\left(\frac{dv}{df'_A}\right)_{f'_A=0} = \left(\frac{v_A}{v^0} - 1\right) \qquad (10)$$

v^0 = specific volume of base glass.
v_A = specific volume constant for component A_mO_n.

Because graphs of $\frac{1}{v^0}\left(\frac{dv}{df'_A}\right)_{f'_A=0}$ versus atomic number would be similar to Figs. 3 and 4, except for changes in the scale of ordinates, such graphs are omitted.

Similar fractional increments can readily be computed for the addition (or subtraction or substitution) of oxide components to any base glass of known properties.

EASTMAN KODAK COMPANY
ROCHESTER, NEW YORK

FUNDAMENTAL PROPERTIES OF SOLUBLE SALTS IN ENAMEL MILL LIQUORS*

BY M. K. BLANCHARD AND A. I. ANDREWS

ABSTRACT

This paper is a summary of the present basic information concerning the individual chemical, physical, and pyrochemical characteristics of the possible, more common soluble constituents present in porcelain enamel slips. The data were chosen with particular regard to their importance in the study of the nature and effect of the various soluble salts on properties of enamel slips and on their drying behavior.

I. Introduction

The study of the properties and film strength of enamel slips has been retarded by the lack of information concerning the possible presence of electrolytes in enamel mill liquors and their relation. A compilation of these data is presented here.

(1) Physical Properties

Table I shows the basic physical characteristics of the various soluble salts, and Figs. 1 to 5 supplement the tabular data and show the salt versus water equilibrium systems for the more important salts. For ease of comparison, these systems have been drawn to the same scale. The diagrams represent the concentration of the stable crystalline phase of each salt in equilibrium with water.

The curve for borax in Fig. 1(*C*), for example, shows that the decahydrate ($Na_2O \cdot 2B_2O_3 \cdot 10H_2O$) is the stable crystalline phase from 0° to 60°C. and that a saturated water solution of this phase exists only at the concentrations and temperatures defined by the curved line relating these two variables. In other words, if between 0° and 60°C. the temperature of a saturated borax solution were lowered below that indicated by the curve, crystalline decahydrated borax would precipitate until equilibrium for the lower temperature would be reached. If the temperature were raised and no additional borax were supplied, a condition of undersaturation would exist.

The decahydrated borax changes at 60° to 62°C. to the pentahydrated form, which is the stable phase in the range of temperature from 60° to 110°C. This

* Presented at the Forty-Fourth Annual Meeting, The American Ceramic Society, Cincinnati, Ohio, April 21, 1942 (Enamel Division). Received October 19, 1943.

TABLE I—BASIC PHYSICAL CHARACTERISTICS OF VARIOUS SOLUBLE SALTS

Compound	Molecular wt.	Melting point (°C.)	Boiling point (°C.)	Specific gravity	Hardness	Crystal form	Color	Refractive index	Solubility: Cold	Solubility: Parts/100	Solubility: Hot
(1) $(NH_4)_2CO_3 \cdot H_2O$ (ammonium carbonate)	114.1	d. 58				Plates	Colorless		$100^{15°}$		
(2) $BaCl_2$ (barium chloride)	208.27	962	1560	3.856		Monoclinic	"		31°	Fig. 4 (*A*)	$59^{100°}$
(3) $BaCl_2 \cdot 2H_2O$	244.31	$-2H_2O$, 100°C.	1560	3.097		"	"	$N_g = 1.660$ $N_p = 1.635$ $N_m = 1.646$	39.3°	" " "	$76.8^{100°}$
(4) $Na_2O \cdot 2B_2O_3 \cdot 10H_2O$ (borax (decahydrate))	381.43	75	$-10H_2O$, 200	1.73		"	White	$\alpha = 1.447$ $\beta = 1.470$ $\gamma = 1.472$	1.3°	Fig. 1 (*C*)	$20.3^{70°}$
(5) $Na_2O \cdot 2B_2O_3 \cdot 5H_2O$ (pentahydrate)	291.35		$-5H_2O$, 200	1.815		Cubic	Colorless		$22^{25°}$	" " "	$52.3^{100°}$
(6) H_3BO_3 (boric acid)	61.8	$-H_2O$, 185°C.		1.435	3	Triclinic	White		$2.66^{0°}$		$40.2^{100°}$
(7) $CaCl_2$ (calcium chloride)	110.99	772	>1600	2.152		Cubic	"	$N = 1.52$	59.5°	Fig. 2 (*B*)	$347^{230°}$
(8) $CaCl_2 \cdot H_2O$	129.01						Colorless		s.†	" " "	s.†
(9) $CaCl_2 \cdot 6H_2O$	219.09	29.92	$-6H_2O$, 200°	1.68		Trigonal	"	$N_g = 1.393$ $N_o = 1.417$	v.s.‡	" " "	v.s.‡
(10) $MgCO_3$ (magnesium carbonate)	84.33	d.* 350		3.037	3.5–4	"	White	$N_g = 1.509$ $N_o = 1.700$	0.01		
(11) $MgCO_3 \cdot 3H_2O$	138.38	$-H_2O$, 100°C.		1.852	2.5	Rhombic	Colorless	$N_g = 1.526$ $N_p = 1.412$ $N_m = 1.501$	$0.15^{15°}$		d.*
(12) $MgSO_4$ (magnesium sulfate)	120.38	1185°		2.66			"		26.9°	Fig. 5 (*B*)	$68.3^{100°}$
(13) $MgSO_4 \cdot 7H_2O$	246.49	d.* 70		1.68		Rhombic	"		72.4°	" " "	$178^{0°}$
(14) $Na_2O \cdot Al_2O_3$ (sodium aluminate)	81.97	1650°				Amorphous			s.†		v.s.‡
(15) $Na_2O \cdot 2B_2O_3$ (borax (anhydrous))	201.27	741		2.367				$N = 1.5147$	1.3°		$8.79^{100°}$
(16) $Na_2O \cdot B_2O_3$ (sodium borate (meta-))	131.63	966	1400°		4–5	Hexagonal prisms		$N_g = 1.461$ $N_o = 1.570$	s.†		v.s.‡
(17) $Na_2O \cdot B_2O_3 \cdot 4H_2O$	203.7	57				Monoclinic			s.†		v.s.‡
(18) Na_2CO_3 (sodium carbonate)	106.00	851	d.*	2.533			White		7.1°	Fig. 2 (*A*)	$48.5^{104°}$
(19) $Na_2CO_3 \cdot H_2O$	124.02		$-H_2O$, 100° C.	1.55	1.5	Rhombic	"	$N_g = 1.524$ $N_p = 1.420$ $N_m = 1.506$	s.†	" " "	s.†
(20) $Na_2CO_3 \cdot 7H_2O$	232.11	d.* 35.1		1.51		Rhombic or trigonal	"		s.†	" " "	s.†
(21) $Na_2CO_3 \cdot 10H_2O$ (sodium carbonate (decahydrate))	286.16			1.46	1–1.5	Monoclinic	"	$N_g = 1.440$ $N_p = 1.405$ $N_m = 1.425$	21.5°	" " "	$238^{34°}$
(22) NaF (sodium fluoride)	42.00	992		2.79		Tetragonal	"	$N_o = 1.3246$ and $N = 1.328$ (artificial)	$4^{18°}$	Fig. 1 (*A*)	
(23) $NaNO_2$ (sodium nitrite)	69.01	271	d.* 320	2.168		Rhombic	Pale yellow		$72.1^{0°}$	Fig. 3 (*B*)	$163.2^{100°}$
(24) $2Na_2O \cdot P_2O_5$ (sodium phosphate (pyro-))	266.03	988		2.45			White		$3.16^{0°}$	Fig. 1 (*B*)	$40.26^{100°}$
(25) $2Na_2O \cdot P_2O_5 \cdot 10H_2O$	446.18	940		1.82		Monoclinic	"		5.4°	" " "	$93^{100°}$
(26) $Na_2O \cdot SiO_2$ (sodium silicate (meta-))	122.05	1088				Orthorhombic	Colorless	$N_g = 1.529$ $N_p = 1.513$ $N_m = 1.518$	s.†		s.d.§
(27) $Na_2O \cdot SiO_2 \cdot 9H_2O$	284.19	47	$-6H_2O$, 100°			Rhombic	"		v.s.‡		v.s.‡
(28) $2Na_2O \cdot SiO_2$ (sodium silicate (ortho-))	184.05	1018				Hexagonal	"				
(29) Na_2SO_4 (sodium sulfate)	142.05	Tr. 500°–hexagonal 884°		2.698	2.7	Orthorhombic	"	$N_g = 1.484$ $N_p = 1.471$ $N_m = 1.477$	s.†	Fig. 5 (*A*)	s.†
(30) $Na_2SO_4 \cdot 7H_2O$	268.16					Tetragonal	"		44.9°	" " "	$202.6^{33°}$
(31) $Na_2SO_4 \cdot 10H_2O$	322.21	d.* 32.4		1.464	1.5–2	Monoclinic	"	$N_g = 1.398$ $N_p = 1.394$ $N_m = 1.396$	12.2°	" " "	$412^{33°}$
(32) $H_2O \cdot SiO_2$ (silicic acid (meta-))	78.08			2.1–2.3		Amorphous	"		i.‖		i.‖
(33) $2H_2O \cdot SiO_2$ (ortho-)	96.09			1.576		"	"		s.s.¶		s.s.¶
(34) NaOH (sodium hydroxide)	40.0	318.4	1390	2.130			White		42°	Fig. 3 (*A*)	$347^{100°}$
(35) $MgCl_2$	95.23	712	1412	2.325		Hexagonal	Colorless		52.8°	Fig. 4 (*B*)	$73^{100°}$
(36) Na_2SiF_6	188.05	d.* 325		2.679		"	White		$0.65^{17.4°}$		$2.46^{100°}$

(34) NaOH (sodium hydroxide)	40.0	318.4	1390	2.325		Hexagonal	Colorless	$0.65^{17.4°}$ $2.46^{166°}$
(35) $MgCl_2$	95.23	712	1412	2.679		"	White	
(36) Na_2SiF_6	188.05	d.* 325						

TABLE I (*concluded*)

Compound	Probable effect on: Clay–water system	Probable effect on: Enamel slip	Mode of addition or source	Ionization products and nature (probable): Primary	Ionization products and nature (probable): Lesser	Ionization products and nature (probable): Character	Decomposition fusion products (probable)
(1) $(NH_4)_2CO_3 \cdot H_2O$ (ammonium carbonate)	Flocculate (?)	(?)	Mill added	NH_4^+ OH^-	$CO_3^=$ H^+	Basic	None
(2) $BaCl_2$ (barium chloride)	Flocculate	Flocculate	Accessory electrolyte	H^+ Ba^{++}	Cl^- OH^-	Acidic	BaO
(3) $BaCl_2 \cdot 2H_2O$	"	"	" "	H^+ Ba^{++}	Cl^- OH^-	"	"
(4) $Na_2O \cdot 2B_2O_3 \cdot 10H_2O$ (borax (decahydrate))	Deflocculate	"	Leached from frit; mill-added or accessory electrolyte	Na^+ OH^-	H^+ $BO_3^=$ or HBO_3^-	Basic	Na_2O, B_2O_3
(5) $Na_2O \cdot 2B_2O_3 \cdot 5H_2O$ (pentahydrate)	"	"	Decahydrate product above 62°C.	Na^+ OH^-	H^+ $BO_3^=$ or HBO_3^-	"	" "
(6) H_2BO_3 (boric acid)	(?)	"	Leached from frit or salt combination product	H^+ $BO_3^=$ or HBO_3^-		Acidic	B_2O_3
(7) $CaCl_2$ (calcium chloride)	Flocculate	"	Accessory electrolyte	Ca^{++} H^+	Cl^- OH^-	"	CaO
(8) $CaCl_2 \cdot H_2O$	"	"	Accessory electrolyte (hydrate)	Ca^{++} H^+	Cl^- OH^-	"	"
(9) $CaCl_2 \cdot 6H_2O$	"	"	Accessory electrolyte (possible hydrate)	Ca^{++} H^+	Cl^- OH^-	"	"
(10) $MgCO_3$ (magnesium carbonate)	"	"	Accessory electrolyte	Mg^{++}	$CO_3^=$ H^+ OH^-	Basic	MgO
(11) $MgCO_3 \cdot 3H_2O$	"	"	Accessory electrolyte (hydrate)	Mg^{++}	$CO_3^=$ H^+ OH^-	"	"
(12) $MgSO_4$ (magnesium sulfate)	"	"	Mill-added or accessory electrolyte	H^+ Mg^{++}	$SO_4^=$ OH^-	Acidic	"
(13) $MgSO_4 \cdot 7H_2O$	"	"	Mill-added or accessory electrolyte (possible hydrate)	H^+ Mg^{+++} Al^{+++} (?) Na^+	$SO_4^=$ OH^- OH^- Al_2O_3 (?)	"	" Na_2O, Al_2O_3
(14) $Na_2O \cdot Al_2O_3$ (sodium aluminate)	"	"					
(15) $Na_2O \cdot 2B_2O_3$ (borax (anhydrous))	Deflocculate	"	Dehydrated borax product	Na^+ OH^-	H^+ $BO_3^=$ or HBO_3^-	Basic	Na_2O, B_2O_3
(16) $Na_2O \cdot B_2O_3$ (sodium borate (meta-))	"	"	Leached from frit or product of leached and added salts	Na^+ OH^-	H^+ $BO_3^=$ or HBO_3^-	"	" "
(17) $Na_2O \cdot B_2O_3 \cdot 4H_2O$		"	Same as No. 16 or possible hydrate	Na^+ OH^-	H^+ $BO_3^=$ or HBO_3^-	"	" "
(18) Na_2CO_3 (sodium carbonate)	"	"	Mill-added or accessory electrolyte derived product	Na^+ OH^-	H^+ $CO_3^=$	"	Na_2O
(19) $Na_2CO_3 \cdot H_2O$	"	"	Mill-added or accessory electrolyte or product of combination of leached and added salts (possible hydrate)	Na^+ OH^- ‖	H^+ $CO_3^=$	"	"
(20) $Na_2CO_3 \cdot 7H_2O$	"	"	Same as No. 19	Na^+ OH^-	H^+ $CO_3^=$	"	"
(21) $Na_2CO_3 \cdot 10H_2O$ (sodium carbonate (decahydrate))	"	"	" " " "	Na^+ OH^-	H^+ $CO_3^=$	"	"
(22) NaF (sodium fluoride)	"	(?)	Leached from frit or combination of leached and added salts	Na^+ H^+ F^-	OH^-	Acidic	NaF
(23) $NaNO_2$ (sodium nitrite)	Flocculate	Flocculate	Mill-added or accessory electrolyte	Na^+ H^+	OH^- NO_2^-	"	Na_2O
(24) $2Na_2O \cdot P_2O_5$ (sodium phosphate (pyro-))	Deflocculate	Deflocculate	Mill added	OH^- Na^+ $PO_4^=$	H^+	Basic**	Na_2O, P_2O_5 (?)
(25) $2Na_2O \cdot P_2O_5 \cdot 10H_2O$	"	"	Mill added (possible hydrate)	OH^- Na^+ $PO_4^=$	H^+	"	" " "
(26) $Na_2O \cdot SiO_2$ (sodium silicate (meta-))	"	Flocculate	Leached salt or product of leached and added salts	Na^+ OH^-	H^+ $SiO_3^=$	"	Na_2O, SiO_2
(27) $Na_2O \cdot SiO_2 \cdot 9H_2O$	"	"	Same as No. 26 (possible hydrate)	Na^+ OH^-	H^+ $SiO_3^=$	"	" "
(28) $2Na_2O \cdot SiO_2$ (sodium silicate (ortho-))	"	"	Same as No. 26 (possible form)	Na^+ OH^-	H^+ $SiO_3^=$	"	" "
(29) Na_2SO_4 (sodium sulfate)	Flocculate (?)	"	Accessory electrolyte or product of leached and added salts	Na^+ H^+	OH^- $SO_4^=$	Acidic**	Na_2O "
(30) $Na_2SO_4 \cdot 7H_2O$	Flocculate	"	Same as No. 29 (possible hydrate)	Na^+ H^+	OH^- $SO_4^=$	"	"
(31) $Na_2SO_4 \cdot 10H_2O$	"	"	Same as No. 30	Na^+ H^+	OH^- $SO_4^=$	"	"
(32) $H_2O \cdot SiO_2$ (silicic acid (meta-))	"	"	Leached from frit	H^+ $SiO_3^=$	OH^-	Acidic	SiO_2
(33) $2H_2O \cdot SiO_2$ (ortho-)	"	"	Leached from frit (possible form)	H^+ $SiO_3^=$	OH^-	"	"
(34) NaOH (sodium hydroxide)	Deflocculate	"	Combination of leached and added materials	Na^+ OH^-		Basic	Na_2O
(35) $MgCl_2$	Flocculate	"	Same as No. 34	Mg^{++} H^+	OH^- Cl^-	Acidic	MgO
(36) Na_2SiF_6	Deflocculate	(?)	Possible leached or derived salt	Na^+ F^-	OH^- H^+		NaF, SiF_4

* d., decomposes. † s., soluble. ‡ v.s., very soluble. § s.d., slight decomposition. ‖ i., insoluble. ¶ s.s. slightly soluble. ** Probable.

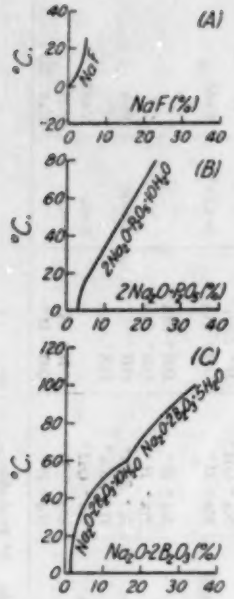

FIG. 1.—(*A*) System $NaF–H_2O$; (*B*) system $2Na_2O{\cdot}P_2O_5–H_2O$; and (*C*) system $Na_2O{\cdot}2B_2O_3–H_2O$.

change from one stable phase to another is clearly shown by the discontinuity in the curve in Fig. 1(*C*).

This system, $Na_2O{\cdot}2B_2O_3–H_2O$, is important because borax is an important component of the crystalline material in a dried porcelain enamel slip. The precise addition of any agent to correct the tearing tendencies contributed by borax cannot be made without careful consideration of the variables related in this diagram.

The data, in general, that are offered by this type of diagram become more valuable when they are used in conjunction with studies of rate and mode of crystallization from solution. Information on the rate of crystal nucleation and growth is important supplementary material.

The remaining diagrams contain the same type of important data, each for a single salt in equilibrium with water. Although the behavior of a salt in the presence of another salt may not be defined by exactly the same curve, the basic behavior, barring chemical changes, may be assumed to be the same.

II. Chemical and Physicochemical Characteristics

(1) Ionization Behavior

The probable ionization behavior of the various soluble salts is listed in Table I. The ionization products are divided into two classes based on the importance of their effect on slip properties. It may be well to note that the Na^+ ion is preponderant and the character of most of the salts is basic.

The ionization behavior of one particular salt in the presence of another cannot be accurately predicted. It is safe, however, to point out that the basic behavior with another salt will probably be altered from the single salt characteristic, barring chemical reactions, only to the extent of the common ion and buffer effects.

(2) Possible Reactions Between Soluble Salts

Table II lists a series of important, possible chemical reactions of the various primary and derived soluble constituents present in a porcelain enamel mill liquor. This series is one small portion of the myriad of reactions that could occur, but only the most obvious possibilities are considered here. These reactions are mainly a straight-forward, double-decomposition type, and no consideration has been given to the nature of the products in relation to their effect on the extent of the reaction.

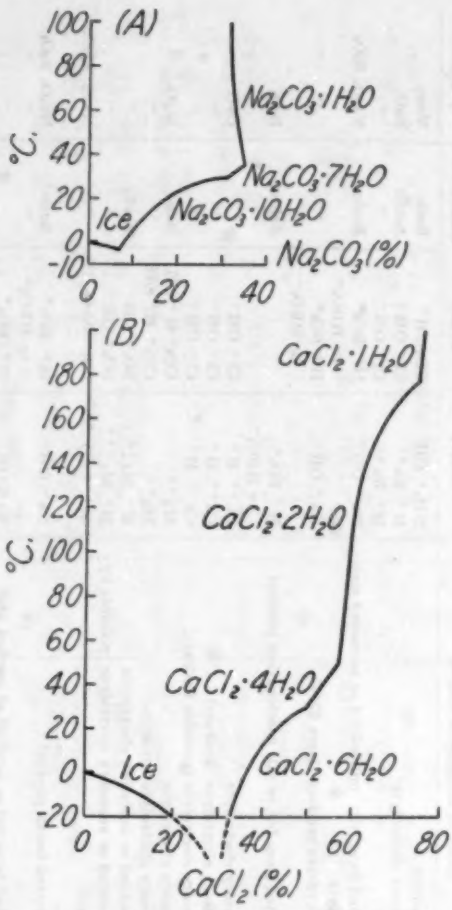

FIG. 2.—(*A*) System $Na_2CO_3–H_2O$; (*B*) system $CaCl_2–H_2O$.

Some of these reactions undoubtedly are important in an enamel mill liquor, and among them are those responsible, at least in part, for the formation of sodium fluoride, sodium metaborate, boric acid, silicic acid, and sodium silicate.

(3) Probable Effect of Various Soluble Salts on Character of Clay–Water Systems

Any effect of a soluble salt on a clay–water system can be said to be the effect of the ionized portion of that salt rather than of the salt itself. The capacity of any salt to affect a clay suspension, other variables being constant, therefore depends on the degree of ionization of that salt in water.

Ion adsorption and base-exchange capacity are terms applied to the physicochemical property of a clay that makes it sensitive to ionized portions of a salt. This property is dependent on the fact that a clay particle has at or near its surface a negative charge that attracts positively charged ions (cations) and holds them at the surface with a tenacity which is a function of the field strength and concentration of the adsorbable ion. One cation may be replaced by another on

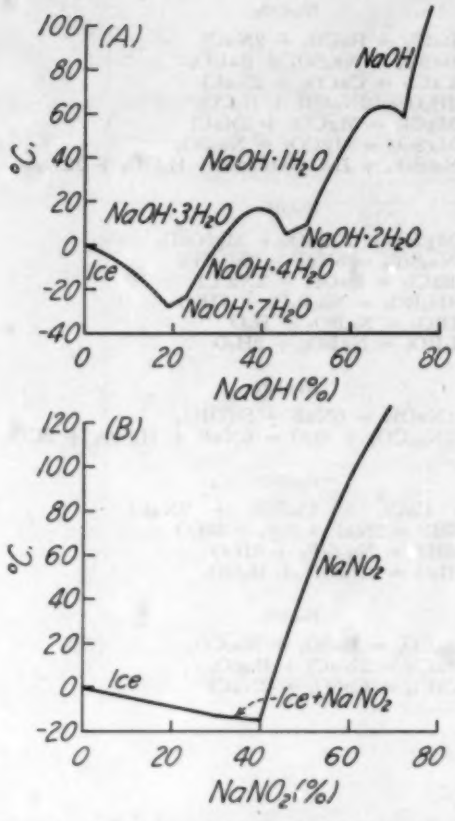

FIG. 3.—(*A*) System $NaOH-H_2O$; (*B*) system $NaNO_2-H_2O$.

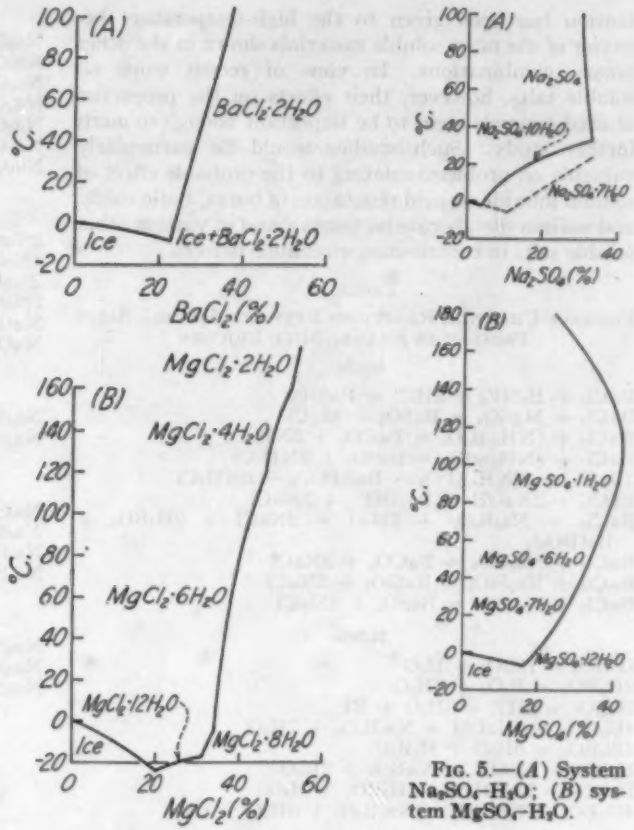

FIG. 4.—(*A*) System $BaCl_2-H_2O$; (*B*) system $MgCl_2-H_2O$.

FIG. 5.—(*A*) System $Na_2SO_4-H_2O$; (*B*) system $MgSO_4-H_2O$.

the clay particle in the clay–water system by exchanging one ion for another in proper concentration. A Na^+ clay (one having Na^+ ions adsorbed on the clay particles), for example, may be made into a H^+ clay simply by leaching the system with an acid.

The effectiveness of the adsorbed cations in flocculating or deflocculating the system depends on the same factors, that is, the field strength and concentration of the adsorbed ion. Small additions of cations which have high field strengths, approximately equal to $\frac{\text{valence}}{\text{ionic radius}}$, will usually flocculate clay–water suspensions. Such ions are H^+, Fe^{+++}, B^{++++}, and Mg^{++}. Small additions of cations which have low field strengths, such as Na^+, K^+, and Li^+, tend to deflocculate clay slips.

The familiar Hofmeister series may be used to illustrate the effects of different cations. The ions in the following series are arranged in the order of increasing flocculating power: Li^+, K^+, Na^+, Rb^+, Cs^+, NH_4^+, Mg^{++}, H^+. Although the left-hand members of this group are considered as deflocculants, the proper addition of any one of them will coagulate a clay–water system. In order to achieve flocculation with these larger, weaker cations, it is necessary to have them present in solution in relatively high concentration.

Using the information of the Hofmeister series, the probable effect of each cation has been predicted in Table I. The preponderant single cation in enamel mill liquors, however, is Na^+. Enamel slips, therefore, probably develop a "set" condition through flocculation by the excessive quantity of Na^+ ions present.

Several of the prominent cations display anomalous characteristics because of the effects of their respective anions. Phosphate, fluoride, and sulfate anions have been notable in their behavior. Little or no actual data on their effects, however, are available, and no generalized statement concerning their combined behavior in enamel slips can therefore be made.

III. Pyrochemical Behavior of Various Soluble Salts Present in Enamel Liquors

(1) The probable fusion products of each of the soluble salts are listed in Table I.

(2) Figures 6 to 10 show binary equilibrium systems of the various primary and derived soluble salts. These data, as stated previously, are by no means indicative of the actual behavior of the same salts in multicomponent systems; they merely represent the behavior of a few of the more important possible combinations.

Of the eleven systems shown, the $Na_2O-B_2O_3$ and Na_2O-SiO_2 diagrams are the only ones in common use by the enamel technologist, and heretofore little at-

tention has been given to the high-temperature behavior of the more soluble materials shown in the other binary combinations. In view of recent work on soluble salts, however, their effects on the properties of fired enamels seem to be important enough to merit further study. Such studies would be particularly valuable on problems relating to the probable effect of sodium fluoride on acid resistance, of borax, boric oxide, and sodium metaborate on tearing, and of various other soluble salts in contributing to enamel defects.

TABLE II

POSSIBLE CHEMICAL REACTIONS BETWEEN SOLUBLE SALTS PRESENT IN ENAMEL MILL LIQUORS

$BaCl_2$

$BaCl_2 + H_2SiF_6 = 2HCl + BaSiF_6$
$BaCl_2 + MgSO_4 = BaSO_4 + MgCl_2$
$BaCl_2 + (NH_4)_2CO_3 = BaCO_3 + 2NH_4Cl$
$BaCl_2 + (NH_4)_2SO_4 = BaSO_4 + 2NH_4Cl$
$3BaCl_2 + 2(NH_4)_3PO_4 = Ba_3(PO_4)_2 + 6NH_4Cl$
$BaCl_2 + 2NaOH = Ba(OH)_2 + 2NaCl$
$BaCl_2 + Na_2B_4O_7 + 3H_2O = 2NaCl + 2H_3BO_3 + Ba(BO_2)_2$
$BaCl_2 + Na_2CO_3 = BaCO_3 + 2NaCl$
$BaCl_2 + Na_2SiO_3 = BaSiO_3 + 2NaCl$
$BaCl_2 + Na_2SO_4 = BaSO_4 + 2NaCl$

H_3BO_3

$H_3BO_3 = HBO_2 + H_2O$
$2H_3BO_3 = B_2O_3 + 3H_2O$
$H_3BO_3 + 3HF = 3H_2O + BF_3$
$4H_3BO_3 + 2NaOH = Na_2B_4O_7 + 7H_2O$
$4H_3BO_3 = 5H_2O + H_2B_4O_7$
$H_3BO_3 + NaOH = NaBO_2 + 2H_2O$
$H_3BO_3 + NaOH = NaH_2BO_3 + H_2O$
$4H_3BO_3 + Na_2CO_3 = Na_2B_4O_7 + 6H_2O + CO_2$

HBO_2

$2HBO_2 = B_2O_3 \cdot H_2O$
$HBO_2 + NaOH = NaBO_2 + H_2O$

B_2O_3

$2B_2O_3 + 2H_2O = 4HBO_2$
$2B_2O_3 + H_2O = H_2B_4O_7$
$2B_2O_3 + 6H_2O = 4H_3BO_3$
$B_2O_3 + 2NaBO_2 = Na_2B_4O_7$
$B_2O_3 + 2NaOH = 2NaBO_2 + H_2O$
$2B_2O_3 + Na_2CO_3 = Na_2B_4O_7 + CO_2$
$B_2O_3 + 3Na_2SO_4 = 3SO_2 + 2Na_2BO_3$
$2B_2O_3 + 12HF = H_3BO_3 + 3H_2O + 3HBF_4$

$CaCl_2$

$CaCl_2 + BaSO_4 = CaSO_4 + BaCl_2$
$3CaCl_2 + H_2SiF_6 + 6NaOH = 3CaF_2 + 6NaCl + Si(OH)_4 + 2H_2O$
$CaCl_2 + 2NaF = CaF_2 + 2NaCl$
$CaCl_2 + 2NaOH = Ca(OH)_2 + 2NaCl$
$CaCl_2 + 2NaAlO_2 = 2\,NaCl + Ca(AlO_2)_2$
$CaCl_2 + Na_2SiO_3 = CaSiO_3 + 2NaCl$
$CaCl_2 + Na_2SO_4 = 2NaCl + CaSO_4$

H_2SiO_3

$H_2SiO_3 = H_2Si_4O + 3H_2O$
$H_2SiO_3 + 2NaOH = Na_2SiO_3 + 2H_2O$
$H_2SiO_3 + Na_2CO_3 = Na_2SiO_3 + H_2CO_3$
$H_2SiO_3 + BaCl_2 = BaSiO_3 + 2HCl$
$H_2SiO_3 + CaCl_2 = CaSiO_3 + 2HCl$
$H_2SiO_3 + Na_2SO_4 = Na_2SiO_3 + H_2SO_4$

$Na_2B_4O_7$

$Na_2B_4O_7 + BaCl_2 + 3H_2O = 2NaCl + 2H_3BO_3 + Ba(BO_2)_2$
$Na_2B_4O_7 + 3H_2O = 2H_3BO_3 + 2NaBO_2$
$Na_2B_4O_7 + 7H_2O = 2NaOH + 4H_3BO_3$
$Na_2B_4O_7 + Na_2CO_3 = 2Na_2B_2O_4 + CO_2$

Na_2CO_3

$Na_2CO_3 + BaCl_2 = BaCO_3 + 2NaCl$
$Na_2CO_3 + BaSO_4 = Na_2SO_4 + BaCO_3$
$Na_2CO_3 + CaCl_2 = CaCO_3 + 2NaCl$
$Na_2CO_3 + 2H_2O = 2NaOH + H_2CO_3$
$Na_2CO_3 + MgCl_2 = MgCO_3 + 2NaCl$
$Na_2CO_3 + MgSO_4 = MgCO_3 + Na_2SO_4$
$Na_2CO_3 + Na_2SiF_6 + H_2O = 6NaF + H_2SiO_3 + 2CO_2$

NaOH

$2NaOH + MgSO_4 = Na_2SO_4 + Mg(OH)_2$
$4NaOH + Na_2SiF_6 = 6NaF + Si(OH)_4$
$2NaOH + BaCl_2 = BaOH + 2Na\,Cl$
$2NaOH + 4H_2BO_3 = Na_2B_4O_7 + 7H_2O$
$NaOH + HBO_2 = NaBO_2 + H_2O$
$NaOH + H_3BO_3 = NaBO_2 + 2H_2O$

Na_2SiF_6

$Na_2SiF_6 + 4NaOH = 6NaF + Si(OH)_4$
$Na_2SiF_6 + 2Na_2CO_3 + H_2O = 6NaF + H_2SiO_3 + 2CO_2$

Na_2SiO_3

$Na_2SiO_3 + CaCl_2 = CaSiO_3 + 2NaCl$
$Na_2SiO_3 + 6HF = 2NaF + SiF_4 + 3H_2O$
$Na_2SiO_3 + 6HF = Na_2SiF_6 + 3H_2O$
$Na_2SiO_3 + H_2O = 2NaOH + H_2SiO_3$

Na_2SO_4

$Na_2SO_4 + BaCO_3 = BaSO_4 + Na_2CO_3$
$Na_2SO_4 + BaCl_2 = 2NaCl + BaSO_4$
$Na_2SO_4 + CaCl_2 = CaSO_4 + 2NaCl$

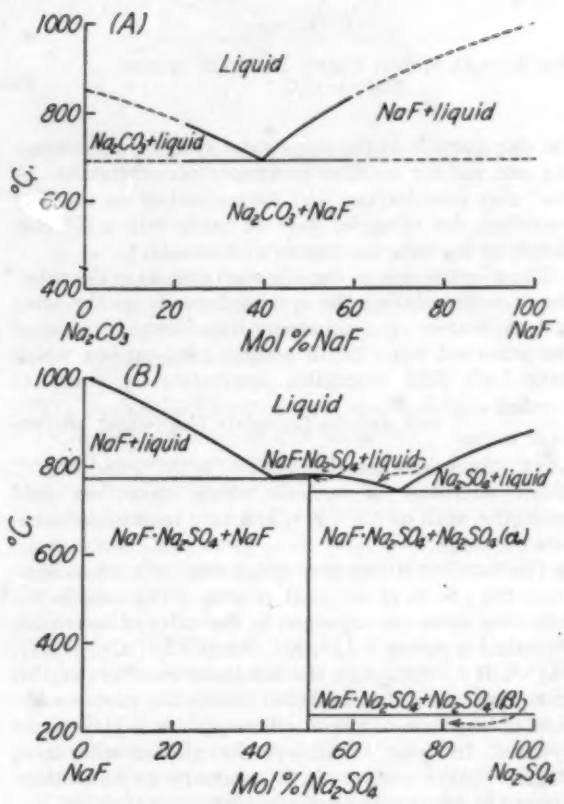

FIG. 6.—(*A*) System Na_2CO_3–NaF; (*B*) NaF–Na_2SO_4.

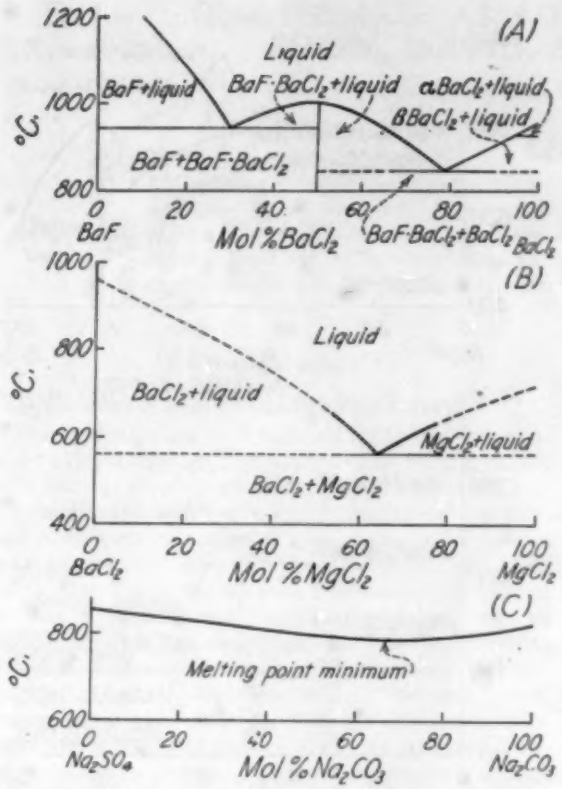

FIG. 7.—(*A*) System BaF–$BaCl_2$; (*B*) system $BaCl_2$–$MgCl_2$; (*C*) system Na_2SO_4–Na_2CO_3.

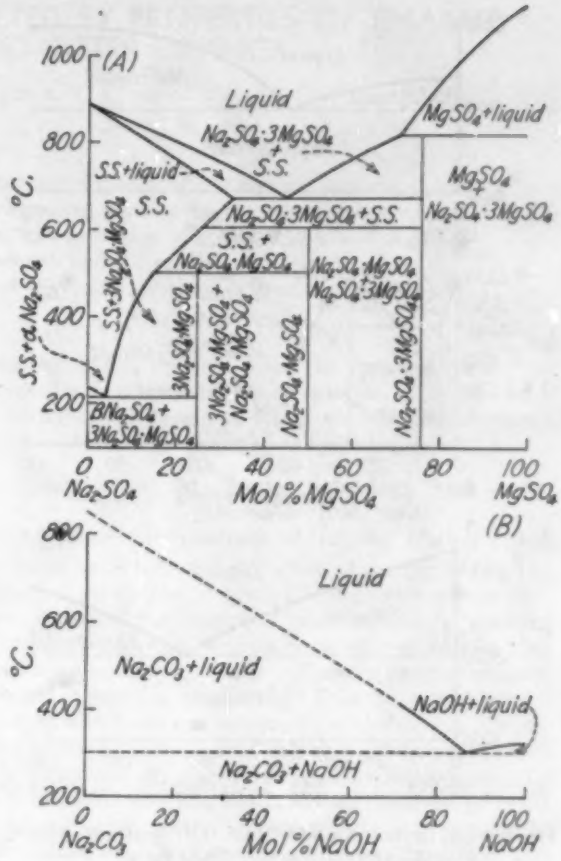

FIG. 8.—(*A*) System Na_2SO_4–$MgSO_4$; (*B*) system Na_2CO_3–NaOH.

Figures 6 (*A*) and (*B*) and 9 (*A*) and (*B*) show NaF in equilibrium with several of the soluble salts. Inasmuch as NaF is the primary crystalline material found in dried enamel mill liquors, it is possible for it to combine with Na_2CO_3, Na_2SO_4, AlF_3, or Na_2SiO_3 in some manner basically resembling the action shown. Sodium carbonate (Na_2CO_3) is shown in combination with two materials, NaOH and Na_2SO_4 (Figs. 8 (*B*) and 7 (*C*)), both of which occur in a mill liquor. Barium chloride, a common electrolyte, is a component of systems with BaF and $MgCl_2$, two possible derived constituents of a mill liquor (Fig. 7 (*A*) and (*B*)). Figures 9 (*C*) and 10 (*A*) and (*B*) show the high-temperature relations of sodium metaborate and sodium metasilicate, sodium oxide and boric oxide, and sodium oxide and silica, all three of which are important in a study of the fusion relations of soluble salts.

IV. Available Data

The following ternary equilibrium systems[1] have been omitted from this report because of the difficulty of simple reproduction:

H_2O–HF–NaF
H_2O–$CaCO_3$–NaCl–Na_2SO_4
H_2O–NH_4Cl–$(NH_4)_2SO_4$
H_2O–NH_4Cl–Na_2SO_4

[1] Annual Tables of Constants and Numerical Data Vol. IV. University of Chicago Press, Chicago, Ill. 1921. 626 pp.

H_2O–$MgCl_2$–$MgSO_4$
H_2O–$MgSO_4$–$CaCl_2$
H_2O–$MgCl_2$–Na_2SO_4
H_2O–$CaCl_2$–Na_2SO_4
H_2O–$NaCl_2$–Na_2SO_4
H_2O–$CaCl_2$–$Ca(NO_3)_2$
H_2O–$BaCl_2$–$Ba(NO_3)_2$
H_2O–$BaCl_2$–$NaNO_3$
H_2O–NH_4Cl–$(NH_4)_2CO_3$
H_2O–NH_4Cl–Na_2CO_3
H_2O–NH_4Cl–$MgCl_2$
H_2O–NH_4Cl–$BaCl_2$
H_2O–NH_4Cl–$(NH_4)_2B_4O_7$
H_2O–NH_4Cl–$Na_2B_4O_7$
H_2O–$MgCO_3$–NaCl
H_2O–NaCl–Na_2CO_3
H_2O–NaOH–NaCl–Na_2CO_3
H_2O–NaCl–$Na_2B_4O_7$
H_2O–$MgCl_2$–$CaCl_2$
H_2O–$MgCl_2$–NaCl
H_2O–$CaCl_2$–Na_2O
H_2O–$BaCl_2$–NaCl
H_2O–$Ba(OH)_2$–NaCl
H_2O–$MgCO_3$–Na_2SO_4
H_2O–Na_2SO_4–Na_2CO_3
H_2O–Na_2SO_4–$Na_2B_4O_7$
H_2O–$MgSO_4$–Na_2SO_4
H_2O–$NaNO_3$–$NaNO_3$
H_2O–$(NH_4)_2B_4O_7$–$Na_2B_4O_7$
H_2O–NaOH–Na_2CO_3
H_2O–H_3BO_3–NaOH

Bibliography

1. A. I. Andrews, Enamels, Twin City Printing Co., Champaign, Ill., 1935. 428 pp.; *Ceram. Abs.*, **14** [7] 158 (1935).
2. H. Landolt and R. Börnstein (revised by W. A. Roth), Physikalisch-Chemische Tabellen. Julius Springer, Berlin, 1923.
3. S. S. Cole, S. R. Scholes, and C. R. Amberg, "Correction in Specific Gravity and Unit Cell Size of Na_2O·B_2O_3," *Jour. Amer. Ceram. Soc.*, **20** [6] 215 (1937).
4. A. M. Comey and D. A. Hahn, Dictionary of Chemical Solubilities. Macmillan Co., 1921.

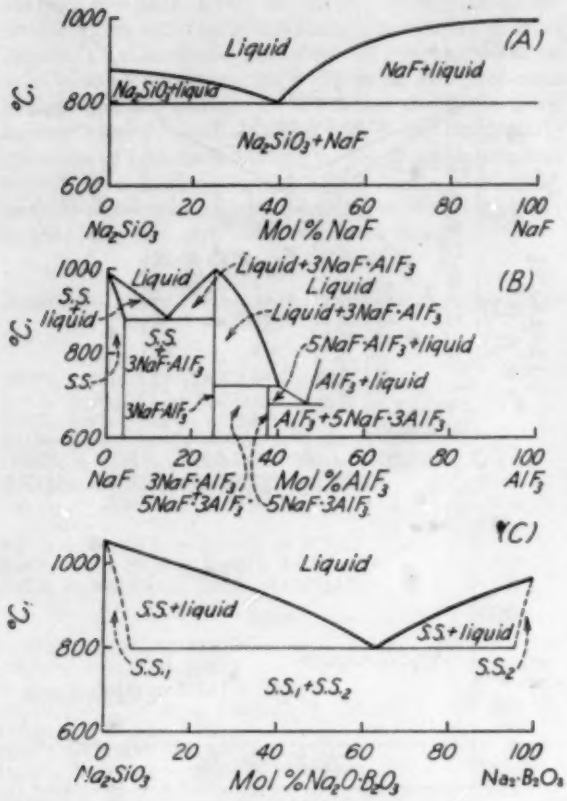

FIG. 9.—(*A*) System Na_2SiO_3–NaF; (*B*) system NaF–AlF_3; (*C*) system Na_2SiO_3–$Na_2O \cdot B_2O_3$.

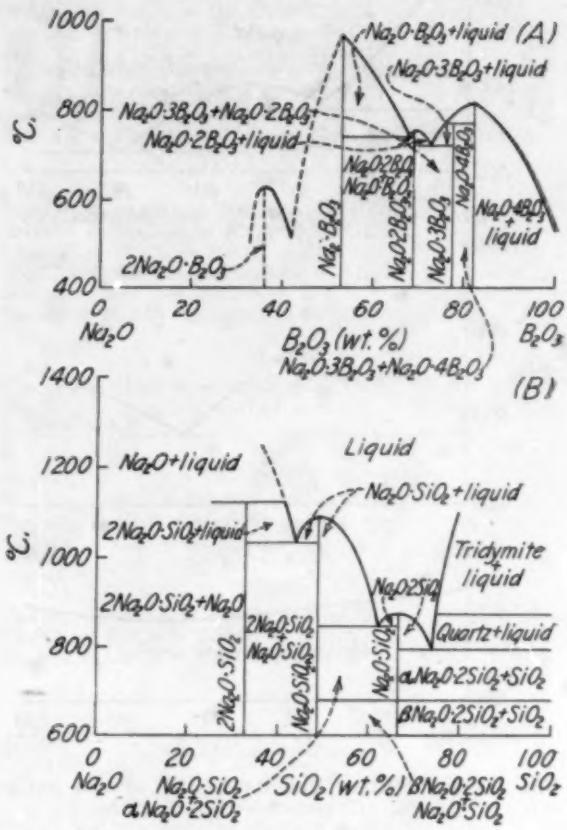

FIG. 10.—(*A*) System Na_2O–B_2O_3; (*B*) Na_2O–SiO_2.

5. Dictionary of Inorganic Chemical Reactions. Edited by M. K. Hoffman and J. A. Barth, 1910.

6. Ssü-Mien Fang, "Crystal Structure of Sodium Metaborate, $NaBO_2$," *Jour. Amer. Ceram. Soc.*, **20** [6] 214 (1937).

7. C. D. Hodgman, Handbook of Chemistry and Physics. Chemical Rubber Pub., 23d ed., 1939. 2221 pp.; *Ceram. Abs.*, **19** [5] 127 (1940).

8. International Critical Tables. Vol. 4, Part 1, pp. 41–97. Vniv. of Chicago Press, 1922.

9. N. A. Lange and G. M. Forker, Handbook of Chemistry and Physics. Handbook Publishers, Inc., Sandusky, Ohio, 1934. xiv + 1265 pp.; *Ceram. Abs.*, **14** [10] 262 (1935).

10. C. E. Marshall, Colloids in Agriculture. Edward Arnold & Co., London, 1935.

11. J. W. Mellor, Comprehensive Treatise on Inorganic and Theoretical Chemistry, Vol. IX. Longmans, Green & Co., Ltd., London, 1929; *Ceram. Abs.*, **8** [5] 373 (1929).

12. A. F. Rogers and P. F. Kerr, Thin Section Mineralogy. McGraw-Hill Book Co., Inc., New York, 1933. 311 pp.; *Ceram. Abs.*, **13** [3] 71 (1934).

13. H. B. Weiser, Colloid Chemistry. John Wiley & Sons, New York, 1939.

14. Hewitt Wilson, Ceramics–Clay Technology. McGraw-Hill Book Co., Inc., New York, 1927. 296 pp.; *Ceram. Abs.*, **6** [11] 547 (1927).

15. A. N. Winchell, "Optic and Microscopic Characters of Artificial Minerals," *Univ. of Wis., Studies in Sci.*, No. 4, Univ. of Wisconsin, Madison, Wis., 1927. 215 pp.; *Ceram. Abs.*, **7** [5] 324 (1928).

Bibliography of Equilibrium Diagrams

(1) Systems given in "Compilations of Phase-Rule Diagrams of Interest to the Ceramist and Silicate Technologist," by Hall and Insley, *Jour. Amer. Ceram. Soc.*, **16** [10] 459–567 (1933); *ibid.*, **21** [4] 113–64 (1938).

System	Fig. No.	System	Fig. No
Na_2SiO_3–NaF	9 (*A*)	Na_2O–B_2O_3	10 (*A*)
NaF–AlF_3	9 (*B*)	Na_2O–SiO_2	10 (*B*)

(2) Systems given in Landolt, Börnstein, and Roth (see reference (2) in Bibliography).

Diagrams or numerical data

System	Fig. No.	System	Fig. No.
NaF–H_2O	1 (*A*)	$MgSO_4$–H_2O	5 (*B*)
$2Na_2O \cdot P_2O_5$–H_2O	1 (*B*)	Na_2CO_3–NaF	6 (*A*)
$Na_2O \cdot 2B_2O_3$–H_2O	1 (*C*)	NaF–Na_2SO_4	6 (*B*)
Na_2CO_3–H_2O	2 (*A*)	BaF–$BaCl_2$	7 (*A*)
$CaCl_2$–H_2O	2 (*B*)	$BaCl_2$–$MgCl_2$	7 (*B*)
NaOH–H_2O	3 (*A*)	Na_2SO_4–Na_2CO_3	7 (*C*)
$NaNO_3$–H_2O	3 (*B*)	Na_2SO_4–$MgSO_4$	8 (*A*)
$BaCl_2$–H_2O	4 (*A*)	Na_2CO_3–NaOH	8 (*B*)
$MgCl_2$–H_2O	4 (*B*)	Na_2SiO_3–$Na_2O \cdot B_2O_3$	9 (*C*)
Na_2SO_4–H_2O	5 (*A*)		

Acknowledgment

The authors wish to express their appreciation to C. G. Harman, Department of Ceramic Engineering, University of Illinois, for his help with data concerning clay–soluble salt–water systems. Appreciation is also extended to the Ferro Enamel Corporation of Cleveland, Ohio, sponsors of the Ferro Enamel Fellowship at the University of Illinois, under which this investigation was made.

DEPARTMENT OF CERAMIC ENGINEERING
UNIVERSITY OF ILLINOIS
URBANA, ILLINOIS

ENAMEL FILM STRENGTH AS AFFECTED BY PROPERTIES OF ENAMEL BEFORE, DURING, AND AFTER DRYING*

By M. K. Blanchard and A. I. Andrews

Abstract

The effect of soluble salts in porcelain enamel mill liquors was investigated, particularly relating to the enamel film strength and tearing tendency. The mechanism of tearing is discussed from the standpoint of the properties of the enamel slip and of dried enamel film. The related data are presented, and the application of the results of recent extensive studies of clay, water, and electrolyte systems to enamel slips is given.

I. Introduction

(1) Purpose of Study and Literature Survey

This investigation was undertaken to add information to the studies on film strength and tearing, which have been a subject of controversy for a long time.

Several authors have reported studies on the relation of the tearing tendency of enamels to the soluble salts in the mill liquor. These investigators[1] have found that the principal salts dissolved from enamel frit are sodium fluoride, sodium carbonate, various sodium borates, and sodium sulfate. Several theories of tearing have been advanced from the results of their studies. Rosenberg and Langerman[1(e)] have attributed tearing to shrinkage of borax during melting, and they claim the function of sodium nitrite to be a mechanical bond for the enamel at a low temperature, holding it together until fusion takes place. Lange[1(g)] agrees with Rosenberg and Langerman that sodium nitrite prevents tearing. Hurst and Andrews[1(f)] show data indicating that tearing is a result of expansion that occurs when boric acid and boric oxide compounds are dehydrated, which ruptures the enamel film. These writers also state that molten boric acid draws together the separate patches of torn enamel to form balls. The mechanism by which sodium nitrite is effective in reducing tearing appears to be the result of the formation of sodium metaborate on reaction with boric acid. Sodium metaborate was found to have little change in volume during dehydration or melting.

II. Procedure and Results

(1) Visual Observations of Tearing During Firing

In order to follow the progress of tearing during the firing of an enamel, a small Chromel wire-wound electric furnace was equipped with a quartz window, through which the samples were viewed with a low-power binocular microscope. The samples were ground-coated squares, approximately 1 in. on a side, spray-coated with cover enamels to 50 gm. per sq. ft. The six test enamels studied were standard white cover coats characteristic of the commercial types in use. To minimize frit solution, the slips were prepared by rapid mixing of clay, water, and electrolyte with previously dry-milled frit. Constant frit fineness (2 gm. from 100 gm. of frit on a No. 200-mesh sieve) and distilled water were used throughout this study; 0.2% of boric acid was added per 100 parts of frit to promote tearing.

These samples were heated, and the observations showed the progress of tearing to be similar in all of the enamels. The first noticeable action was the formation of a series of hairline mud cracks in the surface of the enamel. These ruptures occurred before the specimen had reached a dull red heat. With continued heating, the cracks were widened by the drawing back of the separate patches of cover enamel, which left the ground coat exposed. This exposure of the cracks appeared to be a manifestation of shrinkage in the heated layer, which was accompanied by a lifting of the layer from the ground coat. The next noticeable behavior was a flattening of the lifted layer and a rounding off of the enamel at the edges of the cracks. When fusion occurred, the enamel flowed together again. The melting together in most cases was preceded by the fusion of the cracked edge with the exposed ground coat so that the ground coat showed after fusion. The various steps are diagrammed in Fig. 1.

(2) Cracking in Dry Enamel Films

In the preparation of samples for visual observation, cracks often appeared in the dried pieces. The fact that tearing originates in these cracks was shown by staining them with a suspension of lampblack in acetone. These observations were verified by careful ex-

---

* Presented at the Forty-Fourth Annual Meeting, The American Ceramic Society, Cincinnati, Ohio, April 22, 1942 (Enamel Division). Received October 19, 1942.

Based on a thesis submitted by the senior author as partial fulfillment of the requirements of the degree of Doctor of Philosophy in Engineering and published with the permission of the Graduate School of the University of Illinois. The work was done on a fellowship sponsored by the Ferro Enamel Corporation, Cleveland, Ohio.

[1] (*a*) H. L. Cook, "Note on Solubility of Enamel Frit in Mill Water," *Jour. Amer. Ceram. Soc.*, **10** [5] 339–43 (1927); "Observations on Effect of Various Electrolytes Added to Enamel Suspensions Made With and Without Clay," *ibid.*, **10** [5] 344–46 (1927).

(*b*) R. D. Cooke, "Study of Soluble Salts in Enamels," *ibid.*, **13** [9] 658–61 (1930).

(*c*) R. R. Danielson, "Effect of Soluble Salts on Properties of Enamels," *ibid.*, **12** [8] 538–47 (1929).

(*d*) R. J. Whitesell, "Effect of Soluble Salts on Properties of Enamels," *ibid.*, **20** [3] 72–75 (1937).

(*e*) J. E. Rosenberg and A. F. Langerman, "Tearing of Vitreous Enamels," *ibid.*, **23** [3] 80–86 (1940).

(*f*) T. L. Hurst and A. I. Andrews, "Study of the Effect of Soluble Salts Present in Enamel Mill Liquors," *ibid.*, **24** [5] 171–78 (1941).

(*g*) L. A. Lange, "Effect of Sodium Nitrite in Cover Enamels," *Bull. Amer. Ceram. Soc.*, **18** [10] 360–65 (1939).

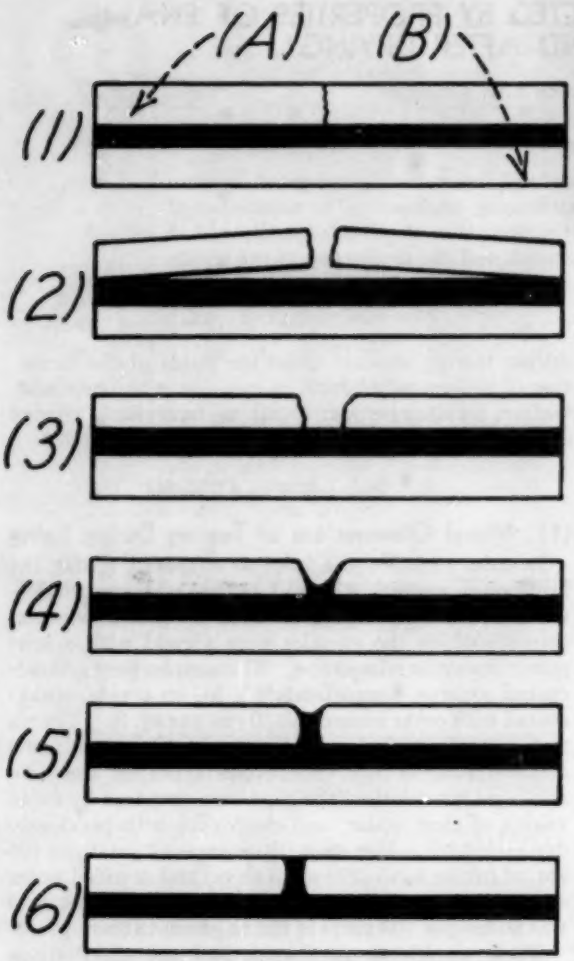

FIG. 1.—Procedure of tearing during firing: (1) beginning of tearing, (*A*) torn cover coat and (*B*) ground-coated steel; (2) shrinkage; (3) completion of shrinkage; (4) fusion; (5) closing of tear; and (6) final enamel.

amination of specimens which had been prepared by spraying them with varying thicknesses of enamels containing boric acid. The cracking, in general, was present in heavily applied enamels (50 to 55 gm. per sq. ft.), but with some of the thinner applications no tearing was evident until the specimen had been heated to 500°F.

(3) Enamel Film Drying Behavior and Shrinkage Characteristics

The cracking noted in the dried enamel films apparently was a manifestation of strain set up in the enamel during drying, which appeared to be a result of the forces of drying shrinkage. The determination of the nature of these strains and their function in the promotion of tearing was the next step in the investigation.

Strips of thin celluloid were coated on one side with enamel slips containing 0.2% of boric acid, and other strips were coated with the same thicknesses of nontearing enamels. Similar slips were also applied on other nonrigid bases, such as tin foil, waxed paper, and

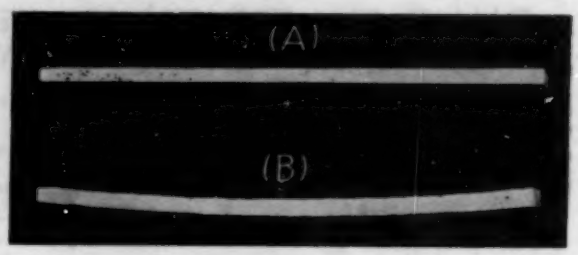

FIG. 2.—Photograph of dried enamels: (*A*) nontearing and (*B*) tearing; note curvature of tearing enamel.

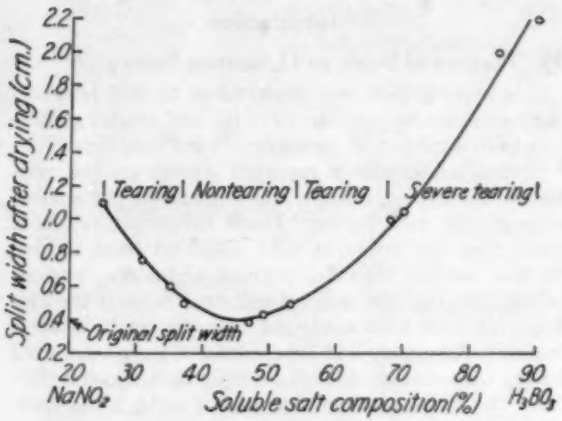

FIG. 3.—Effect of soluble salt composition on enamel drying shrinkage as measured by the strain set up in split rings of shim stock coated with enamel.

varying thicknesses of brass shim stock. The results were the same in all cases. Those enamels containing boric acid bent during drying so that the base assumed a curvature in which the ends were higher than the middle; the degree of bend was determined by the relative rigidities of the base materials. The nontearing enamels remained flat throughout the drying procedure.

The shrinkage characteristics were also examined by preparing samples of tearing and nontearing enamels. The slip was dried in a mold that was placed on a greased glass surface to prevent adherence of the enamel. The drying behavior of these specimens was similar to previous results in which the tearing enamel assumed a curvature and the nontearing layer remained flat (Fig. 2).

The foregoing visual data were supplemented by measurements of the relative strains set up in split rings of shim stock while the enamel coatings were drying. Enamels that contained H_3BO_3 and $NaNO_2$ in the combinations shown in Fig. 3 were sprayed to a thickness of 45 gm. per sq. ft. on 2-in. diameter split rings of 0.01-in. shim stock, which were 1 in. wide and had an original gap width of 0.4 cm. The enamels were prepared by wet milling, and 1% of total electrolyte was added to each slip. The increase in gap widths after drying was measured as a criterion of tensile strain set up in the enamel during drying. To check these measurements against the tearing character of the enamels, the same slips were sprayed and fired on

ground-coated pieces. The results of these experiments are shown in Fig. 3. Wet-milled enamels showed the same characteristics when total quantities of H_3BO_3 and $NaNO_2$ as low as 0.2% were added to the slips.

These experiments revealed the behavior of good and bad enamels during drying on surfaces on which shrinkage strains were relieved by warping and bending. When these enamels were applied on rigid bases to which they adhered, the release of strain in tearing was brought about by the cracking, which is fundamentally responsible for tearing.

The observed strains were affected by a difference in total drying shrinkage between good and poor enamels or by a shrinkage gradient in the poor enamel. A shrinkage gradient exists in an enamel coating if the surface shrinks and becomes hard before the remainder of the enamel is dry. Careful measurements of several tearing and nontearing enamels showed the volume drying shrinkages to be approximately 35%, with a range of not more than 2% between good and poor enamels. This difference in total shrinkage is not enough to account for the degree of bending, warping, or cracking that was observed.

The sole difference in tearing and nontearing enamels on nonrigid bases therefore appears to occur as a result of the manner in which drying shrinkage takes place. The shrinkage in the poor enamel is stepwise so that surface curling and cracking take place before internal drying is complete. The good enamel has practically the same shrinkage, but the drying character is such that the shrinkage is uniform throughout the whole layer. When the same enamels are applied on rigid surfaces, the differential drying stresses of the poor enamels are absorbed by surface cracking followed by internal cracking along the same ruptures so that the surface crack penetrates the entire enamel layer. The enamel that does not tear has no strain gradient; the over-all strains, however, obviously have been relieved by other means inasmuch as the total shrinkage is also high in this enamel.

(4) Textural Properties of Enamel Films

Because there are differences in the surface characteristics of dried enamel films, a study was made of the textural characteristics and their relation to film strength and resistance to the forces of shrinkage. The method of study was simple. Thin sections were cut in various directions from dried samples of tearing and nontearing enamels. Each slip was divided into two parts; 0.2% of H_3BO_3 was added to one part and 0.2% of $NaNO_2$ to the other. This procedure gave samples of tearing and nontearing enamels that were sprayed on ground-coated specimens and poured into molds on a greased glass plate. The dried enamels were broken from the pieces and were saturated in Canada balsam to prevent slaking during grinding of the thin sections. Photomicrographs of several of these samples are presented in Figs. 4 and 5.

Figure 4 (*A*) and (*B*) shows magnified sections cut perpendicular to the surfaces of a tearing and a nontearing enamel, which had been applied at a thickness

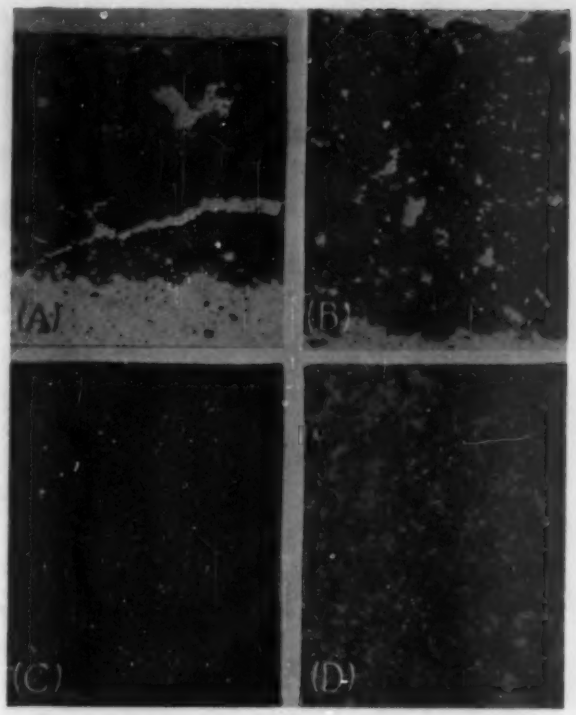

FIG. 4.—(*A*) and (*B*), thin sections cut perpendicular to dry surfaces of an enamel normally applied; (*C*) and (*D*), thin sections cut parallel to surfaces of enamels used in sections shown in (*A*) and (*B*); (*A*) and (*C*) tearing and (*B*) and (*D*) nontearing enamels.

of 50 gm. per sq. ft. These cross sections show clearly the textural differences in a tearing and a nontearing enamel. The good enamel is loosely packed and has an open network of pores. The poor enamel shows a gradation of density from the surface down with no loose packing near the top surface. The more porous texture is near the bottom. Figure 4 (*C*) and (*D*) shows the differences in surface texture more clearly because the specimens were cut parallel to the surfaces of those used for Fig. 4 (*A*) and (*B*). The sections of Fig. 5 were prepared from perpendicular and parallel sections, respectively, of two thick enamels, one containing H_3BO_3 and the other $NaNO_2$. The textural differences again are apparent, with the good enamel revealing an open, loose structure as compared with that of the poor enamel.

These two sets of enamels, prepared from different frits, were characteristic of a number of sections examined with the microscope. The same result occurred in every case and showed conclusively the differences in textural and packing characteristics of tearing and nontearing enamels in the dry state. The density of surface and near surface packing of the tearing enamels shows the cause of the drying behavior. The capacity for more dense packing and the finer pore structure hinder drying so that the shrinkage gradient is effective in setting up tearing stresses. Careful measurements of water loss versus time for tearing and nontearing enamels substantiate this conclusion because

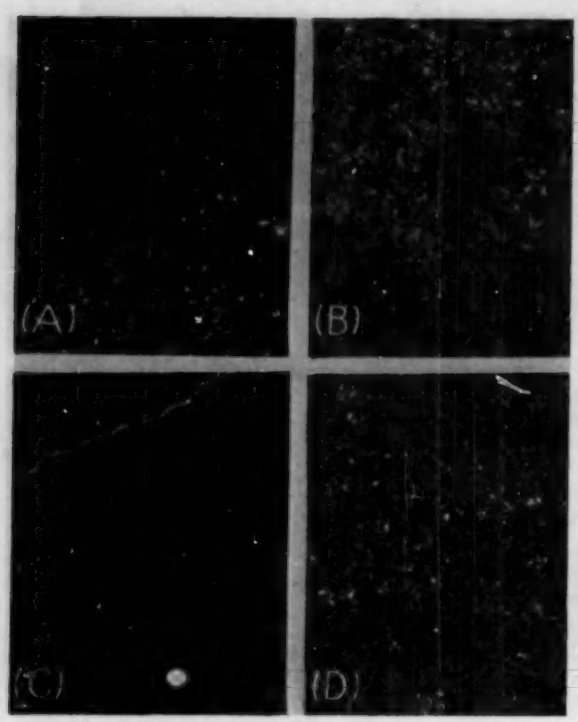

FIG. 5.—(*A*) and (*B*), thin sections cut perpendicular to dry surfaces of very thick (*A*) tearing enamel and (*B*) nontearing enamel; (*C*) tearing and (*D*) nontearing thin sections of enamels cut parallel to surfaces of enamels used in sections shown in (*A*) and (*B*).

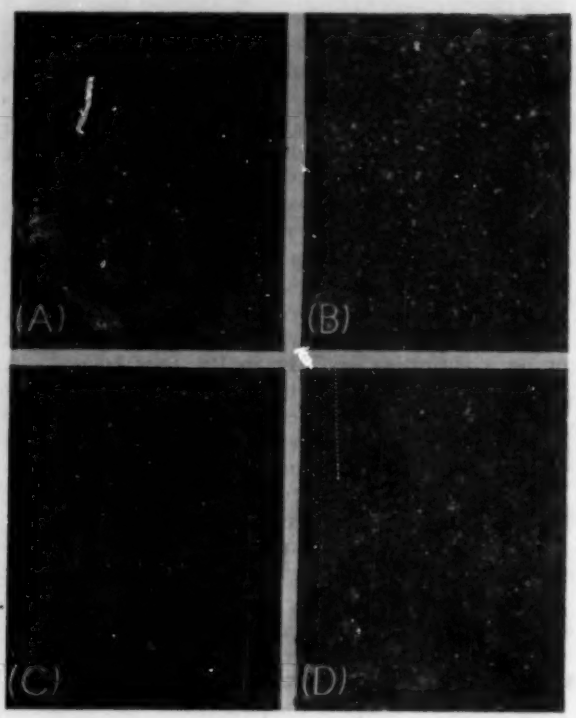

FIG. 6.—Thin sections cut perpendicular to surfaces of calcined enamels, (*A*) tearing and (*B*) nontearing types; thin sections of calcined enamels (*C*) and (*D*) cut parallel to surfaces of enamels used in sections shown in (*A*) and (*B*).

the nontearing enamel dries more quickly than the tearing enamel.

The nontearing enamels, moreover, have an open structure essential to even drying and even shrinkage. The good enamels are also capable of absorbing shrinkage stress, even or uneven, because of their networks of large, open pores. The film strength of the nontearing enamel appears in effect to be "film weakness," inasmuch as cracking that would free the stress in a dense enamel occurs as a single tear whereas this stress could be absorbed by a multiplicity of small cracks in the loosely packed enamel. An extreme example has been noted many times in this study in which the forces binding together the densely packed surface layer in a tearing enamel were so great that release of stress was brought about by the release of the enamel layer from the ground coat. Firing stresses were released later by the shrinkage of the enamel as a unit rather than in small patches away from mud cracks. The film strength, or actual bond strength between packed particles, was greater in this case than the force holding the enamel to the ground coat.

To complete the study, the effect of additional heating on the enamel textures was investigated. Using the same types of samples as before, thin sections were made of enamels which had been calcined to 1000°F. for ten minutes. Photomicrographs of thin sections cut perpendicular and parallel to surfaces of calcined tearing and nontearing enamels are shown in Fig. 6.

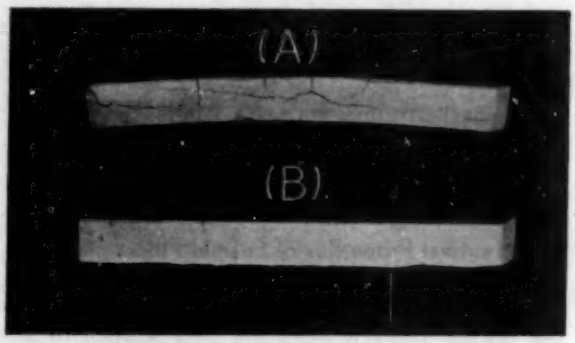

FIG. 7.—Photograph of calcined, thick sections of enamels (*A*) tearing and (*B*) nontearing; note curvature of tearing enamel.

The characteristics of these sections were not distinctly different from those of the dry enamels discussed in section II. All of the tearing enamels became more densely packed, whereas the nontearing enamels retained the loose character observed in the dry state except that further shrinkage took place with the additional heating. Figure 7 shows the relative behavior of the tearing and the nontearing enamels after they were heated to calcining temperatures. The curved specimen is typical of a tearing enamel. Shrinkage has progressed in both samples, but the surface and near-surface shrinkage of the poor enamel is greater than that of the good enamel. The surface of the

tearing enamel was very hard, and close packing appeared to have taken place to at least one-half the depth of the sample. The nontearing sample, however, was comparatively soft and homogeneous throughout. The effect of shrinkage is again clearly demonstrated, and the difference in packing characteristics of tearing and nontearing enamels is further emphasized. The density of the more tightly packed enamel simply increases, that is, the surface shrinkage increases more than that of the interior to a degree equivalent to the difference that existed after drying. The nontearing enamel shrinks uniformly and maintains an open structure. If the enamels had adhered to a rigid surface, the dense enamel would have been subjected to stress release by forming large cracks and the loosely packed enamel would have absorbed the same shrinkage in the myriad of smaller cracks between grains in the loose structure.

(5) Chemical and Physicochemical Effects Responsible for Packing Characteristics

This study has shown that the shrinkage behavior and the physical character of the enamel are responsible for low film resistance to the tearing tendency. Both characteristics have been shown to be manifestations of the packing density of the dried enamel film. The soluble salts and their concentrations were the only variables allowed to enter and must therefore determine the packing character. The mechanism of packing, accordingly, was investigated.

In a system in which clay is in contact with water, the first effect of soluble-salt additions depends on the kind and amount of ions in solution that are furnished to the system. This ionic content thus governs the degree of dispersion or coagulation of the clay portion of that system and, other things being equal, fixes the suspending power of the clay by fixing the states of aggregation of the clay fraction in the system. For a given water content, a coagulated clay makes a "thick" slip and a dispersed clay makes a "thin" slip; the thicker slip, however, has the better suspending power for an added nonplastic.

The physicochemical property of a clay that is responsible for its ability to assume varying degrees of aggregation is based on its characteristic capacity to adsorb ions. The clay particle has a negative charge at or near its surface that attracts positively charged ions (cations) and holds them with a tenacity which is a function of the electrical field strengths and concentration of the cations in solution. One cation may be exchanged for another on the clay particle by exchanging the type of ion in the surrounding solution. A Na^+ clay, for example, may be made into a H^+ clay simply by leaching the clay with an acid. Small amounts of cations with high field strengths, in general, will coagulate clay-water suspensions; such ions are H^+, Fe^{+++}, Mg^{++}, and Ba^{++}. Small additions of cations with low field strengths, such as Na^+, K^+, and Li^+, tend to disperse clay slips, that is, to make them thin and fluid. If larger quantities of these low field strength ions are added to clay slips, they coagulate after the first cycle of dispersion. Curve (1) of Fig. 8 shows this effect on the pickup of a slip of clay, quartz, and water to which varying amounts of NaOH have been added.

An enamel slip is essentially one in which frit is suspended in clay and water. The ordinary water content is such that the system is mobile or "thin" when the clay fraction is dispersed. If the clay is coagulated properly, the slip is said to be "set up." The Na^+ ion is preponderant in the enamel mill liquors, resulting from frit solution, and the action of this sodium ion in an enamel slip is to bring about the second cycle coagulation already described. Curve (2) in Fig. 8 shows the relation of viscosity to salt concentration for a clay, quartz, and water slip to which concentrated mill liquor from a nontearing frit has been added. There is a marked similarity in the curves; curve (1) represents the slip containing NaOH and curve (2), the actual mill liquor. The first few portions of NaOH disperse the slip, which allows the flint to settle out and destroys the suspension; more NaOH gives the slip a normal, good set; and further additions thicken it to such a degree that it is no longer usable. The addition of concentrated mill liquor (0.64 gm. of solid per cc. of mill liquor) from a nontearing enamel gave the slip the same characteristics as the NaOH but not to the same degree. The region of best set as shown in Fig. 8 is in the trough of the mill liquor curve, and the NaOH additions at the trough give an exceedingly thin slip. The slip containing the mill liquor is not coagulated completely in the region of good set as compared with the ends of the curve. This mill liquor slip is coagulated, however, in relation to the NaOH slip at the trough. The differences in trough depths of the curves are the result of sodium salts in the mill liquor which buffer the action of Na^+ at a higher level and thus prevent the primary dipersion resulting from the addition of a single base, such as NaOH. Most important among these salts are NaF, $Na_2B_4O_7 \cdot 10H_2O$, Na_2SO_4, $Na_2O \cdot B_2O_3$, Na_2CO_3, and $Na_2O \cdot SiO_2$.

The conditions of dispersion and coagulation used in these studies are entirely relative and may be present in varying degrees, as shown by Fig. 8. The slip containing mill liquor, if considered by itself, has three distinct regions, two of relative coagulation and one of relative dispersion. The NaOH slip has the same three regions but the action of the single, highly ionized

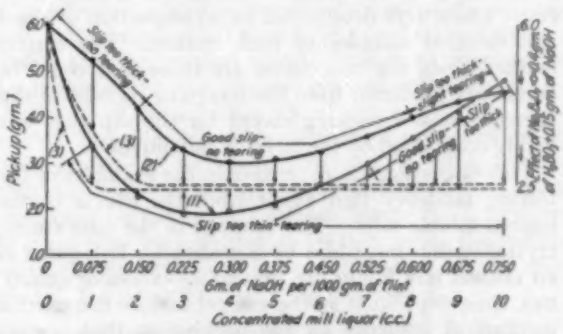

FIG. 8.—Effect of NaOH and mill liquor additions on consistency of slips of flint (100), clay (6) and water (40); curve (1) NaOH additions; (2) mill liquor additions; and (3) consistency shift effected by 0.04% of H_3BO_3.

base is such that the degree of dispersion at the trough is high enough to render the slip too thin. The salts contained in the mill liquor are ionized so that the degree of dispersion at the trough is actually a degree of coagulation when compared with the NaOH slip. The trough values, in other words, are simply relative points between two extreme end members with one closer than the other to a condition of complete coagulation. The good set of an enamel slip cannot be correctly termed an absolute state of coagulation but simply a high degree of coagulation. The terms, "coagulation" and "dispersion," will be used hereafter in this paper to connote the degree of the condition rather than the absolute state itself.

The difference between a dispersed slip and a coagulated slip in relation to the finer fraction depends on the state of aggregation of the clay particles. A coagulated slip, for example, is one in which numerous clay particles are bound together in a porous, soft, water-containing cluster; in the dispersed system, these clay particles remain as separate entities, each surrounded by a water film and each free to move without hindrance from the other members of the system. With this simple picture, it is clear how the two states of aggregation affect the packing character of drying slips. The coagulated system, for example, made up of ten clusters of a hundred particles each will pack during drying so that the ten clusters touch and have between them large pore spaces and relatively few points of contact between clusters. The same slip, if dispersed, will consist of a thousand separate particles free to pack with a much finer system of pores.

The fine pore size of the dispersed slip makes the drying more difficult with a consequent strain incurred by the existence of a moisture gradient. The same packing character, with the numerous contact points and high strength, makes the absorption of this strain more difficult because the separate particles cannot be pulled apart easily, and large cracks can occur only when the concentrated strain over an area becomes strong enough to break the forces between particles. The loosely packed system, however, dries with no moisture gradient, and the forces between the clusters of frit and clay are weak enough to permit the release of over-all drying strain. Figure 8 shows the condition of the slips and resultant effects on the tearing tendency, which were determined by an inspection of dried and calcined samples of each enamel. The results marked along the two curves are those that could be accurately predicted from the foregoing concept of slip aggregation and packing except for the slip that was highly coagulated by the 10 cc. of mill liquor.

This discussion has covered only the examples of the tearing tendency that result from the effects of the ionized soluble salts. The behavior of the salts during crystallization must also be considered. If borates in an enamel mill liquor are present in excessive quantities, their deposition at the enamel surface can exert a mechanical influence on the packing so that tearing occurs. An example of this extreme case was furnished by the slip of Fig. 8, which had been coagulated by a 10-cc. addition of mill liquor from a nontearing enamel. This addition, however, furnished two and one-half times the quantity of salts ordinarily found in the mill liquor from which the concentrated additions used previously were prepared.

(6) Effect of Specific Salts on Tearing

Boric acid has long been considered to be the principal cause of tearing, and the addition of H_3BO_3 to an enamel slip invariably causes a reduction in resistance to rupture. The addition of this weak acid to the slips used for the data of Fig. 8 had a characteristic effect on the properties of the slips, which gives ample ground for a discussion of the effect of H_3BO_3 additions to porcelain enamels.

The dotted lines of Fig. 8 show the effect of a 0.04% H_3BO_3 addition on consistency and tearing resistance of the NaOH and mill liquor slips. A slight reduction of viscosity occurs when no NaOH or mill liquor is present; small additions decrease the viscosity rapidly and the slips are thin over the remainder of the field. Tearing occurs, as indicated in Fig. 8, over almost the entire range. The slip containing mill liquor has been dispersed to a greater degree over its total length, and the NaOH slip has been dispersed in two regions and relatively coagulated in the trough region. The logical explanation for this action is that it may be assumed to be the result of chemical reaction with the materials already present in solution in the slips. The resultant chemical compound shows all of the attributes of a buffering salt because further additions of NaOH or mill liquor have no effect over the range studied. The ionization of Na from the buffering compound is such that the amount of ions free to fix the slip consistency is constant.

The minimum value of consistency is achieved at approximately 0.15 gm. of NaOH, the quantity that is theoretically necessary to form $Na_2B_4O_7 \cdot 10H_2O$ on reaction with H_3BO_3. As a check, the amount of borax (0.61 gm.) that would be formed in this reaction was added to a slip containing no soluble salt, and the effect on consistency is shown on the right in Fig. 8. This experimental reasoning does not prove that the buffering salt is borax. The evidence, however, makes it clear that the compound is a borate which fixes the Na^+ ion concentration at a level that disperses this type of slip to give it the packing characteristics that result in tearing.

The action is probably the same in enamel slips. If the composition of the frit is such that the resultant soluble salt approaches the borax composition, tearing will result. If H_3BO_3 is added to a normal enamel, the equilibrium between Na^+ and OH^-, CO_3^{--}, SO_4^{--}, F^-, borate$^-$, or other anions present will be shifted so that the dispersion reaches the point at which tearing begins. The normal enamel mill liquor is buffered with an effective Na^+ ion concentration that is higher than the concentration allowed when the H_3BO_3 is added so that not enough ions are available to maintain the proper degree of slip coagulation. To re-establish this proper equilibrium, the Na^+ ion concentration may be raised by adding enough ionizable sodium salt to re-press the buffer completely and

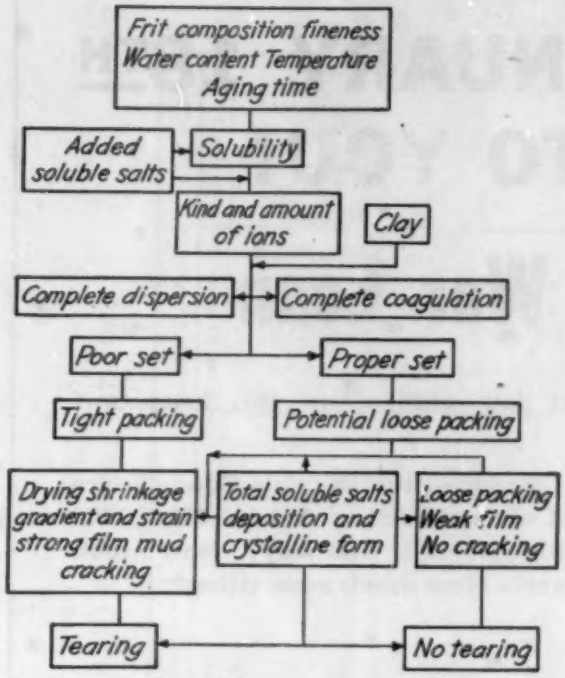

FIG. 9.—Relation of variables determining tearing tendency.

to have sufficient excess remaining for proper slip coagulation. The buffer action may be nullified in this manner by the addition of any of several sodium salts. The sodium salts that were effective[1(f)] were $NaNO_2$, NaOH, Na_2CO_3, $NaNO_3$, $NaBO_2$, and NaCN. Some other sodium salts of lower solubility and lower ionizability reduced the tearing tendency. Among these salts were sodium oxalate, sodium citrate, sodium molybdate, and sodium fluoride. Some of these salts are undesirable because of their blistering tendency during firing, which is caused by decomposition during heating. The quantities necessary to establish the proper equilibrium depend on their solubility and ionization. Less NaOH is required, for example, than $NaNO_2$ or NaCN, and less Na_2CO_3 is required than sodium citrate or sodium oxalate.

Other salts that react favorably in increasing the effective Na^+ ion concentration and in giving final compounds with the proper solubility are those that have a character similar to sodium. Among them are $ZnBO_2$, $Zn(NO_3)_2$, $LiNO_3$, and $Pb(NO_3)_2$. These compounds are effective in reducing the tearing tendency, but they are not used because of unfavorable behavior during decomposition. They are cited merely to illustrate the fact that salts other than sodium are effective in stopping tearing. The sodium salts are not unique in their behavior, and if the composition of enamel frits yielded something as a soluble product other than the sodium borates, the same conditions of tearing could be produced and remedied entirely without their use. Salts of boron have long been considered to be marked in their capacity to produce tearing, but this is true only because enamel frits are compounded of soluble borates. A boron-free enamel has been prepared by the authors and has been found to tear as badly as any normal enamel to which H_3BO_3 has been added.

(7) Effect of Firing on Enamel Films

As has been pointed out previously, the firing treatment seems to have the effect of increasing any film defect that exists after drying is complete. If the packing nature of the dry enamel is such that drying strain has been introduced, with or without release, the firing treatment and consequent shrinkage appear to augment these to the degree that would be expected. The mode and nature of crystallization of the various soluble salts are probably most important in this capacity. Hurst and Andrews[1(f)] have discussed the melted viscosities of the various salts during fusion; they report that heating increases the tearing tendency and that the separate patches of torn enamel are drawn away from the previously formed ruptures.

III. Summary

The results of this investigation may be summarized in a flow sheet in which the various properties and conditions governing these properties are related to the characteristics studied. Figure 9 lists each variable in the sequence considered logical in this study.

IV. Conclusions

Observations of the results of this study offer the following conclusions:

(1) Enamel tearing is a defect caused by shrinkage stresses set up in an enamel film during drying and early firing combined with the inability of the film to absorb these stresses properly.

(2) The capacity of a nontearing enamel to resist tearing depends on the absence of a strain gradient during drying as well as on a loose, weak texture.

(3) The packing character of the enamel during drying affects the characteristic shrinkage and resultant strain gradient in a tearing enamel.

(4) This packing character is determined primarily by the state of aggregation of the enamel slip according to the kind and quantity of adsorbed ions present. The ion most effective in enamel slips is the Na^+ ion freed on solution of frit glass. The final state of aggregation of a dry enamel is influenced in extreme cases by the total quantity, disposition, and crystalline characteristics of the soluble salts present.

(5) The addition of boric acid to an enamel slip causes tearing by forming a buffer salt (probably borax) that disperses the slip and permits it to pack so that strain and tearing result. Sodium nitrite and a number of other salts prevent tearing by re-pressing the buffer and balancing the Na^+ ion concentration to give the enamel the proper packing characteristics.

DEPARTMENT OF CERAMIC ENGINEERING
UNIVERSITY OF ILLINOIS
URBANA, ILLINOIS

STARTING JANUARY 18TH
IT'S UP TO YOU!

The Fourth War Loan

How will American business—how will you—profit from this important campaign? Here's how!

1. **$24,000,000,000.00 of "E, F and G" Bonds—"the People's Bonds"—are already in the safety deposit boxes of our Nation. $24,000,000,000.00! How much building and automobile steel will that buy? How much brisk business energy will that create? How much advertising?**

   Isn't that important to you?

2. **At this moment, War Bonds relieve the high pressure of scarce consumer goods buying by pumping excess income out of the inflationary blood stream.**

   Isn't that important to you?

3. **War Bonds enable the Government to buy war matériel out of increased earnings instead of through created bank funds. That's the way every thinking business man—every other thinking American—wants it.**

   Isn't that important to you?

4. **War Bonds tend to stabilize the economic flow so that slippery peaks of war-time overactivity are smoothed and carried over to equalize the valleys of possible future employment slack. That's mighty important to business.**

   Isn't that important to you?

5. **War Bonds build national morale by giving every American a chance to share in war-financing. Many War Bond owners had never seen bonds before. Now they own a share in America!**

   Isn't that important to you?

The American Ceramic Society, Incorporated

OFFICIAL PERSONNEL OF DIVISIONS AND CLASSES, 1943–1944

	Design	Enamel	Glass	Materials and Equipment	Refractories	Structural Clay Products	White Wares
Trustee	C. W. Read	R. L. Fellows	G. W. Morey	J. E. Eagle	J. B. Austin	Frederick Heath, Jr.	F. P. Hall
Chairman	W. A. Weldon	D. G. Bennett	J. F. Greene	E. M. Rupp	C. L. Thompson	L. R. Whitaker	J. R. Beam
Vice-Chairman	Theodore Lenchner	H. D. Carter	K. C. Lyon	J. R. Kauffman	W. R. Kerr	C. P. Austin	
Secretary	Myrtle M. French	D. G. Moore	S. R. Scholes	J. F. Day	S. M. Swain	R. L. Stone	J. W. Whittemore
Division Nominations	J. P. Thorley	F. R. Porter M. J. Bahnsen E. E. Howe	E. W. Tillotson U. E. Bowes R. A. Miller	S. S. Cole J. F. McMahon	R. S. Bradley P. G. Herold	J. H. Isenhour W. C. McGolpin J. G. Seanor	Donald Hagar R. E. Gould
Papers and Program	H. E. Simpson Rexford Newcomb, Jr.	H. D. Carter	K. C. Lyon	V. J. Roehm	E. E. Callinan C. L. Norton, Jr. E. B. Read C. A. Freeman	V. W. Boeker A. C. Jackson H. K. Lynn	C. M. Lambe, Jr. E. P. McNamara
Membership	Theodore Lenchner	J. F. Hunt	R. R. Shively	D. E. Walsh	G. B. Remmey S. F. Walton W. P. Charbonnier A. R. Blackburn	R. R. Robinson A. C. Christopher	John D. Clark
Standards		R. L. Cook W. N. Harrison W. W. Higgins R. M. King F. A. Petersen	F. W. Adams H. P. Hood K. M. Henry	J. S. Breitenstein		E. F. Theobald A. W. Hough	F. P. Hall
Research		J. C. Reimers	H. R. Lillie Alexander Silverman W. R. Lester	R. R. Robinson	D. W. Ross	H. C. Plummer H. G. Schurecht	*Ball clay:* Ralston Russell, Jr. *Steatite:* Glenn Howatt
Classification and Nomenclature	Mrs. J. W. Dixon	G. H. McIntyre	E. P. McNamara	R. G. Janatka	C. M. Dodd	C. F. Wiseman R. E. Grim Morriss Corbman	A. S. Watts J. R. Beam Ralston Russell, Jr. Harry Thiemecke E. K. Koos
Rules		W. A. Deringer	S. R. Scholes	Philip Dressler	S. F. Walton	Howells Frechette	Don Postlewaite
Councillors		J. D. Tetrick Karl Kautz	F. C. Flint R. W. Wampler	V. V. Kelsey		R. A. Shipley C. F. Tefft	
Exhibitions			J. E. Frazier				
Industrial Management			C. J. Uhrmann	C. L. Cruikshank	O. L. Jones	J. C. Peck	A. A. Wells
Bibliography		J. E. Rosenberg					

	Institute of Ceramic Engineers	Ceramic Educational Council
President	H. B. DuBois	R. M. Campbell
Vice-President	R. F. Sherwood	C. M. Dodd
Secretary	Karl Schwartzwalder	E. C. Henry

THE AMERICAN CERAMIC SOCIETY TRUSTEES AND OFFICERS FOR 1943–1944

President: C. E. Bales, Ironton Fire Brick Co., Ironton, Ohio.
Vice-President: E. H. Fritz, Stupakoff Ceramic & Mfg. Co., Latrobe, Pa.
Treasurer: C. Forrest Tefft, The Claycraft Co., Columbus, Ohio
Secretary-Editor: R. C. Purdy, 2525 North High St., Columbus, Ohio
Past-President: L. J. Trostel, General Refractories Co., Baltimore, Md.
Past-President: J. T. Littleton, Corning Glass Works, Corning, N. Y.

TRUSTEES FROM INDUSTRIAL DIVISIONS*

Design: C. W. Read, Shenango Pottery Co., New Castle, Pa. (1946)
Enamel: R. L. Fellows, Chicago Vitreous Enamel Product Co., Cicero, Ill. (1946)
Glass: G. W. Morey, Geophysical Laboratory, Washington, D. C. (1944)
Materials and Equipment: J. E. Eagle, 6306 20th Ave., Green Meadows, Hyattsville, Md. (1945)
Refractories: J. B. Austin, U. S. Steel Corp., Kearny, N. J. (1946)
Structural Clay Products: Frederick Heath, Jr., Owens-Corning Fiberglas Corp., Toledo, Ohio (1945)
White Wares: F. P. Hall, Onondaga Pottery Co., Syracuse, N. Y. (1944)
Institute of Ceramic Engineers: H. G. Wolfram, Pemco Corp., Baltimore, Md. (1944)
Ceramic Educational Council: J. W. Whittemore, Virginia Polytechnic Institute, Blacksburg, Va. (1944)

* Date of expiration of term of office in parentheses.

DIVISION OFFICERS

Design
Chairman: W. A. Weldon, Locke Insulator Corp., Baltimore, Md.
Secretary: Myrtle M. French, Art Institute of Chicago, Chicago, Ill.

Enamel
Chairman: D. G. Bennett, University of Illinois, Urbana, Ill.
Secretary: D. G. Moore, National Bureau of Standards, Washington, D. C.

Glass
Chairman: J. F. Greene, Kimble Glass Co., Vineland, N. J.
Secretary: S. R. Scholes, N. Y. State College of Ceramics, Alfred, N. Y.

Materials and Equipment
Chairman: E. M. Rupp, Yancey Cyanite Co., Burnsville, N. C.
Secretary: J. F. Day, Donald Hagar Ceramic Materials, Zanesville, Ohio

Refractories
Chairman: C. L. Thompson, Harbison-Walker Refractories Co., Pittsburgh, Pa.
Secretary: S. M. Swain, North American Refractories Co., Cleveland, Ohio

Structural Clay Products
Chairman: L. R. Whitaker, Carolina Ceramics, Inc., Columbia, S. C.
Secretary: R. L. Stone, Dept. of Ceramic Engineering, Univ. of North Carolina, Raleigh, N. C.

White Wares
Chairman: J. R. Beam, Universal Sanitary Mfg. Co., New Castle, Pa.
Secretary: J. W. Whittemore, Virginia Polytechnic Institute, Blacksburg, Va.

OFFICERS OF THE FELLOWS

Dean: R. B. Sosman, U. S. Steel Corp., Kearny, N. J.
Associate Dean: Howells Frechette, Bureau of Mines, Ottawa, Ontario, Canada.
Secretary-Treasurer: R. M. King, Ohio State University, Columbus, Ohio

INSTITUTE OF CERAMIC ENGINEERS

President: H. B. DuBois, Consolidated Feldspar Corp., Trenton, N. J.
Vice-President: R. F. Sherwood, United Feldspar & Minerals Corp., New York, N. Y.
Secretary: Karl Schwartzwalder, A C Spark Plug Co., Flint, Mich.

CERAMIC EDUCATIONAL COUNCIL

President: R. M. Campbell, N. Y. State College of Ceramics, Alfred, N. Y.
Vice-President: C. M. Dodd, Iowa State College, Ames, Iowa
Secretary: E. C. Henry, Pennsylvania State College, State College, Pa.

LOCAL SECTIONS

Baltimore-Washington
Chairman: D. G. Moore, National Bureau of Standards, Washington, D. C.
Secretary: J. C. Richmond, National Bureau of Standards, Washington, D. C.

Central Ohio
Chairman: H. J. Orlowski, O.S.U. Engr. Expt. Sta., Columbus, Ohio
Secretary: A. C. Jackson, The Claycraft Co., Columbus, Ohio

Chicago
Chairman: Hugo Filippi, 228 N. LaSalle St., Chicago, Ill.
Secretary: J. J. Svec, Industrial Publications, Inc., 59 E. VanBuren St., Chicago, Ill.

Michigan-Northwestern Ohio
Chairman: J. F. Quirk, AC Spark Plug Co., Flint, Mich.
Secretary: W. V. Blake, Macklin Co., Jackson, Mich.

Northern California
President: W. V. Bragdon, California Faience Co., Berkeley, Calif.
Secretary: P. C. Valentine, Del Monte Properties Co., San Francisco, Calif.

Pacific-Northwest
President: Howard Mansur, Washington Brick & Lime Co., Spokane, Wash.
Secretary: J. A. Pask, Univ. of Washington, Seattle, Wash.

Pittsburgh
Chairman: W. C. Rueckel, Koppers Co., Pittsburgh, Pa.
Secretary: J. W. Jordan, Mellon Institute, Pittsburgh, Pa.

Southern California
Chairman: R. H. Martin, Vernon Kilns, Los Angeles, Calif.
Secretary: W. O. Brandt, Gladding, McBean & Co., Los Angeles, Calif.

St. Louis
Chairman: H. H. Hanna, Pittsburgh Plate Glass Co., Crystal City, Mo.
Secretary: J. H. Ivery, Hydraulic Press Brick Co., St. Louis, Mo.